



Article

AMPK Is the Crucial Target for the CDK4/6 Inhibitors Mediated Therapeutic Responses in PANC-1 and MIA PaCa-2 Pancreatic Cancer Cell Lines

Bortecine Sevgin ^{1,†}, Merve Nur Coban ^{1,†}, Özge Rencuzogullari ¹, Ajda Coker-Gurkan ², Pinar Obakan-Yerlikaya ¹, Pinar Uysal Onganer ³ and Elif Damla Arisan ^{4,*}

¹ Department of Molecular Biology and Genetics, Atakoy Campus, Istanbul Kultur University, 34156 Istanbul, Turkey; bortecinesevgin@gmail.com (B.S.); mervenercobann@gmail.com (M.N.C.); o.berrak@iku.edu.tr (Ö.R.); p.obakan@iku.edu.tr (P.O.-Y.)

² Department of Molecular Biology and Genetics, Biruni University, 34010 Istanbul, Turkey; a.coker@biruni.edu.tr

³ Cancer Research Group, School of Life Sciences, College of Liberal Arts and Sciences, University of Westminster, 115 New Cavendish Street, London W1W 6UW, UK; P.onganer@westminster.ac.uk

⁴ Institute of Biotechnology, Gebze Technical University, 41400 Gebze, Turkey

* Correspondence: d.arisan@gtu.edu.tr

† These authors contributed equally to this work.



Citation: Sevgin, B.; Coban, M.N.; Rencuzogullari, Ö.; Coker-Gurkan, A.; Obakan-Yerlikaya, P.; Uysal Onganer, P.; Arisan, E.D. AMPK Is the Crucial Target for the CDK4/6 Inhibitors Mediated Therapeutic Responses in PANC-1 and MIA PaCa-2 Pancreatic Cancer Cell Lines. *Stresses* **2021**, *1*, 48–68. <https://doi.org/10.3390/stresses1010005>

Received: 19 January 2021

Accepted: 23 February 2021

Published: 18 March 2021

Publisher's Note: MDPI stays neutral with regard to jurisdictional claims in published maps and institutional affiliations.



Copyright: © 2021 by the authors. Licensee MDPI, Basel, Switzerland. This article is an open access article distributed under the terms and conditions of the Creative Commons Attribution (CC BY) license (<https://creativecommons.org/licenses/by/4.0/>).

Abstract: The survival rate of pancreatic ductal adenocarcinoma (PDAC) patients is short, and PDAC is a cancer type that ranks fourth in the statistics regarding death due to cancer. Mutation in the KRAS gene, which plays a role in pancreatic cancer development, activates the PI3K/AKT/mTOR signaling pathway. The activity of the AMPK as a cellular energy sensor is one of the fundamental mechanisms that can induce effective therapeutic responses against CDK4/6 inhibitors via adjusting the cellular and tumor microenvironment stress management. The phosphorylation of AMPK α at the different phosphorylation residues such as Thr172 and Ser 377 causes metabolic differentiation in the cells following CDK4/6 inhibitor treatment in accordance with an increased cell cycle arrest and senescence under the control of different cellular players. In this study, we examined the competencies of the CDK4/6 inhibitors LY2835219 and PD-0332991 on the mechanism of cell survival and death based on AMPK signaling. Both CDK4/6 inhibitors LY2835219 and PD-0332991 modulated different molecular players on the PI3K/AKT/mTOR and AMPK signaling axis in different ways to reduce cell survival in a cell type dependent manner. These drugs are potential inducers of apoptosis and senescence that can alter the therapeutic efficacy cells.

Keywords: pancreatic ductal adenocarcinoma; PD-0332991; LY2835219; PI3K/AKT/mTOR and AMPK signaling axis; cell cycle

1. Introduction

Pancreatic ductal adenocarcinoma (PDAC) is the most prevalent type of pancreatic cancer that accounts for about 85% of pancreatic tumors. PDAC is the ninth most common cancer in women and the tenth most common cancer in men. It is also the fourth leading cause of cancer death [1]. In pancreatic cancer patients, 70% of whom are between the ages of 55 and 84 and mostly men [2,3], the mutation in the oncogene KRAS (proto-oncogene, GTPase) gene, which plays a role in the development of PDAC, activates the Cyclin-Dependent Kinases (CDK) and the mTOR signaling pathway associated with increased cell survival [4,5]. Molecular profiling studies have shown that KRAS mutations and the CDK inhibitor 2A (CDKN2A or INK 4A/ARF), a tumor suppressor gene, is inactivated in PDAC. The CDKN2A gene encodes the p16INK4a protein, a potent inhibitor of CDK4 and CDK6 [6,7]. The loss of CDK2NA (p16) and tumor suppressor TP53 in the cell cycle causes uncontrolled cell proliferation. Moreover, accumulating

mutations in KRAS, TP53, MYC (myelocytomatosis oncogene cellular homologous), and LKB1 (liver kinase B1) play a role in glucose metabolism, which affects cell maintenance [5,8–10]. Therefore, altered metabolic machinery in PDAC cells is promising to find a new cure for successful disease management. LKB1 acts as a master upstream kinase directly phosphorylating AMP-activated protein kinase (AMPK), defined as a well-known regulator of cellular energy homeostasis. The LKB1-AMPK pathway serves as a metabolic checkpoint in the cell, arresting cell growth in low intracellular nutrient and ATP levels, which is crucial for cancer prognosis [11,12]. Furthermore, CDK4 is activated in the disrupted cell cycle to inhibit AMPK activity via direct phosphorylation of the AMPK- α 2 subunit [13,14]. Therefore, changes in the activity of AMPK play an essential role in tumor aggressiveness [15,16]. The decreased AMPK activity has been also shown to increase pancreatic cancer invasion and metastasis through the Heat Shock Protein -1 (HSF1)-dependent manner [17]. The PI3K/AKT/mTOR pathway plays a critical role in controlling cell growth, proliferation, migration, and metabolism [18–20]. PI3K signaling negatively regulates phosphatase and tensin homolog (PTEN), which is altered in most cancers, including pancreatic cancer [20,21]. PTEN also acts as a tumor suppressor gene by exhibiting phosphatase protein activity. AMPK inhibits the PI3K/AKT/mTOR signaling to reduce cell proliferation through the attenuation of Cyclin D, CDK4, and CDK6 levels [22–24]. The activation of upstream mitogenic pathways that increase CDK4/6 activity creates resistance to therapy in most tumor types [25,26]. Therefore, the continuous activation of the cell cycle and related signaling pathways has enabled the use of CDK inhibitors as an effective therapeutic agents in cancer treatment [27].

Palbociclib (PD 0332991) and abemaciclib (LY2835219), known as the CDK4/6 inhibitors, are the therapeutic agents used in the treatment of advanced metastatic hormone receptor-positive (HR+)/HER2-negative breast cancer [28–30]. The effects of these small molecule inhibitors are investigated in many types of malignancies as they are essential in the regulation of various signaling mechanisms, either alone or combined therapy regimes [28]. LY2835219, which has a similar structural property to PD-0332991, is remarkable for crossing the blood brain barrier. Trials are ongoing to evaluate LY2835219 in cancer patients with brain metastases [31]. LY2835219 binds competitively to CDK4 and CDK6 at the ATP binding site and has been found to exhibit 14 times more specific critical inhibition activity compared to PD 0332991 [32]. It was reported in hepatocellular carcinoma that palbociclib induced the AMPK activity independently of CDK4/6 [33]. Mostly, CDK4 is accepted as the new metabolic sensor that antagonizes AMPK to mediate a metabolic switch. For this purpose, the CDK4/6 inhibitor mediated downstream metabolic alteration related to AMPK is important for understanding the drug responsiveness in different cancer cells. AMPK activation mediated mTORC1 inhibition possess essential role in the regulation of replicative senescence in different cell lines [34]. It is also well described that PD-0332991 and LY2835219 have been shown to prevent the phosphorylation of the retinoblastoma (RB) protein, a well-known tumor suppressor, thereby invoking cancer cell cycle arrest at the G1 phase [27,30,35,36]. Almost all CDK4/6 inhibitors have been shown to induce apoptosis in several types of tumors and are associated with canonical effects such as cell cycle inhibition and proliferation [29,37–39]. LY-2535219 and PD-0332991 have recently revealed new non-canonical functions, inducing reversible senescence, metabolic rearrangement, and immunomodulation [39,40]. The activation of senescence may be a promising novel approach for cancer treatment [41,42].

This study evaluated the therapeutic potential of CDK4/6 inhibitors based on differential AMPK activation status in PANC-1 and MIA PaCa-2 cells with different genetic and biological features. Both cells had homozygous deletions of *CDKN2A* and were highly metastatic. The expression level of PI3K and AMPK was higher in MIA PaCa-2 cells than PANC-1 cells [43]. Therefore, the effect of both CDK inhibitors LY-2535219 and PD-0332991 on the inhibition of cell proliferation was determined through

PI3K/AKT/mTOR/AMPK signaling axis and senescence mechanism in pancreatic cancer cells.

2. Results

2.1. CDK4/6 Inhibitors Reduced Cell Viability and Proliferation in a Dose-Dependent Manner

To examine the effect of LY2835219 and PD-0332991 on relative cell viability and colony-forming ability in PANC-1 and MIA PaCa-2 PDAC cells, we used MTT and colony formation assays.

PANC-1 and MIA PaCa-2 cells were treated with LY2835219 and PD-0332991 at 0.5, 1, 1.5, 2, 2.5, 3, 3.5, 4, 4.5, 5, 7.5 and 10 μM concentrations for 24 h. We found that increasing concentrations of LY2835219 and PD-0332991 decreased cell viability in a dose-dependent manner in PANC-1 and MIA PaCa-2 cells (Figure 1A,B). Low concentration of LY2835219 such as 1 μM and 2 μM treatment caused a significant decrease in cell viability by 50% ($50 \pm 1.4\%$; $n = 4$; $p < 0.001$) PANC-1 cell lines. Moreover, MIA PaCa-2 cells were more sensitive, and 1 μM and 2 μM treatment of LY2835219 further decreased cell viability by 50% and 70%, respectively. Therefore, the IC₅₀ values of LY2835219 were 2 μM and 1 μM in PANC-1 and MIA PaCa-2 cells, respectively. Similarly, 2 μM and 3 μM PD-0332991 treatment reduced cell viability by 50% ($50 \pm 1.3\%$; $n = 4$; $p < 0.001$) in PANC-1 and MIA PaCa-2 cells [29,44,45]. The IC₅₀ values of PD-0332991 were 2 μM for both PANC-1 and MIA PaCa-2 cells. A gradual decrease in both PANC-1 and MIA PaCa-2 cells' cell viability was noted after the incubation with LY2835219 or PD-0332991. However, neither PD-0332991 nor LY2835219 treatment exerted any significant effect on the reduction of cell viability of normal non-tumorigenic human pancreatic ductal epithelial (HPDE) cells (Figure 1C). Therefore, we conducted a colony-forming test to examine the long-term effects of LY2835219 and PD-0332991 with 1, 1.5, 2, 2.5 and 3 μM concentrations for 24 h (Figure 1D). The dose-dependent experiments of both CDK inhibitors were performed to observe the cytotoxic potential of a higher concentration of drugs. The colony formation analysis was terminated after untreated cells were reached in confluent colony numbers and usually it took 14 days. Therefore, the colony formation tests were biologically repeated at least two times. In line with the MTT assay results, LY2835219 showed a more effective therapeutic effect in suppressing the colony formation in MIA PaCa-2 and PANC-1 cells. It was determined that PD-0332991 showed a partial therapeutic effect (Figure 1D). 1 μM LY2835219 remarkably reduced the potential of colony formation of each cell line. However, PD-0332991 treatment exerted various effects on the colony formation capacity of PANC-1 and MIA PaCa-2. Although PANC-1 cells showed higher colony numbers than MIA PaCa-2 cells, 2 and 3 μM concentrations of PD-0332991 treatment reduced the colony numbers of PANC-1 cells by 25% and MIA PaCa-2 cells by 15% and 20%, respectively. Thus, 1 and 2 μM treatments of LY2835219 and 2 and 3 PD-0332991 concentrations were selected for further experiments in PANC-1 and MIA PaCa-2 cells.

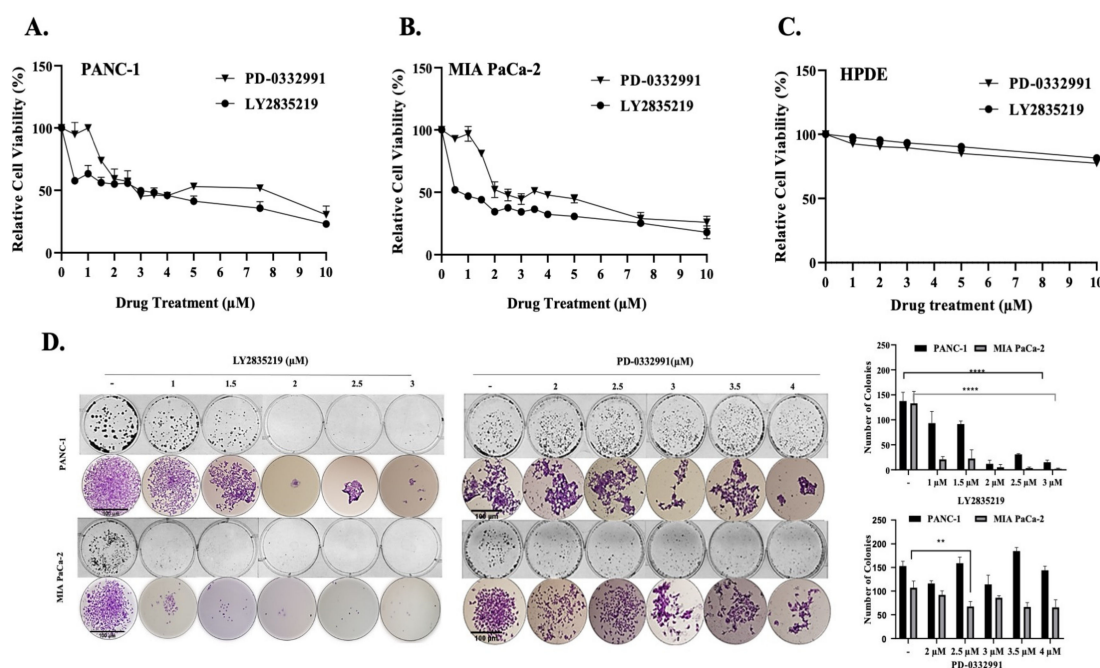


Figure 1. LY2835219 and PD-0332991 decreased cell viability in PANC-1 and MIA PaCa-2 cells. (A) PANC-1 (B) MIA PaCa-2, (C) human pancreatic ductal epithelial (HPDE) cells (1×10^4) were treated with LY2835219 and PD-0332991 (0–10 μM) for 24 h. Cells were incubated for 24 h with drug doses and analyzed by the 3-(4,5-dimethylthiazol-2-yl)-2,5-diphenyltetrazolium bromide (MTT) method. The data are the means \pm SD of at least five different experiments evaluated by 2-way ANOVA and Bonferroni's multiple comparison test. (D) PANC-1 and MIA PaCa-2 cells were exposed to 1, 1.5, 2, 2.5 and 3 μM of LY2835219 and PD-0332991 for 24 h. Then, the colony formation of cells was counted after 14 days of treatment with media replenishment every 2 days. The histograms represented the mean \pm SD of 2 separate experiments. Scale bar is 100 μm . ** $p < 0.01$; **** $p < 0.0001$.

2.2. LY2835219 and PD-0332991 Arrest the Cell Cycle and Led to Senescence

Flow cytometry was used to examine the effect of LY2835219 and PD-0332991 on the cell cycle progression in PDAC cell lines. To evaluate the effect of the drugs on cell cycle distribution, we treated PANC-1 and MIA PaCa-2 cells with increasing doses for 24 h. In the PANC-1 cell line, we observed that LY2835219 treatment increased the G1 phase retention rate in a dose-dependent manner. This rate has been shown to affect a population of 62.8% after 2 μM LY2835219 treatment. However, we have observed that increasing doses of LY2835219 treatment does not cause a significant arrest in the cell cycle in MIA PaCa-2 cell line (Figure 2A). As shown in Figure 2B, 2 μM and 3 μM doses of PD-0332991 treatment resulted in cell cycle G1 arrest in 89% ($88.1 \pm 1.3\%$; $n = 2$; $p < 0.001$) and 87% ($86.7 \pm 1.8\%$; $n = 2$; $p < 0.001$), respectively, compared to the control group. A similar result was observed in the MIA PaCa-2 cell line. 2 μM and 3 μM doses of PD-0332991 treatment induced G1 phase arrest in 93% ($92.9 \pm 1.5\%$; $n = 2$; $p < 0.001$) and 95% ($95.4 \pm 1.8\%$; $n = 2$; $p < 0.001$), respectively (Figure 2B).

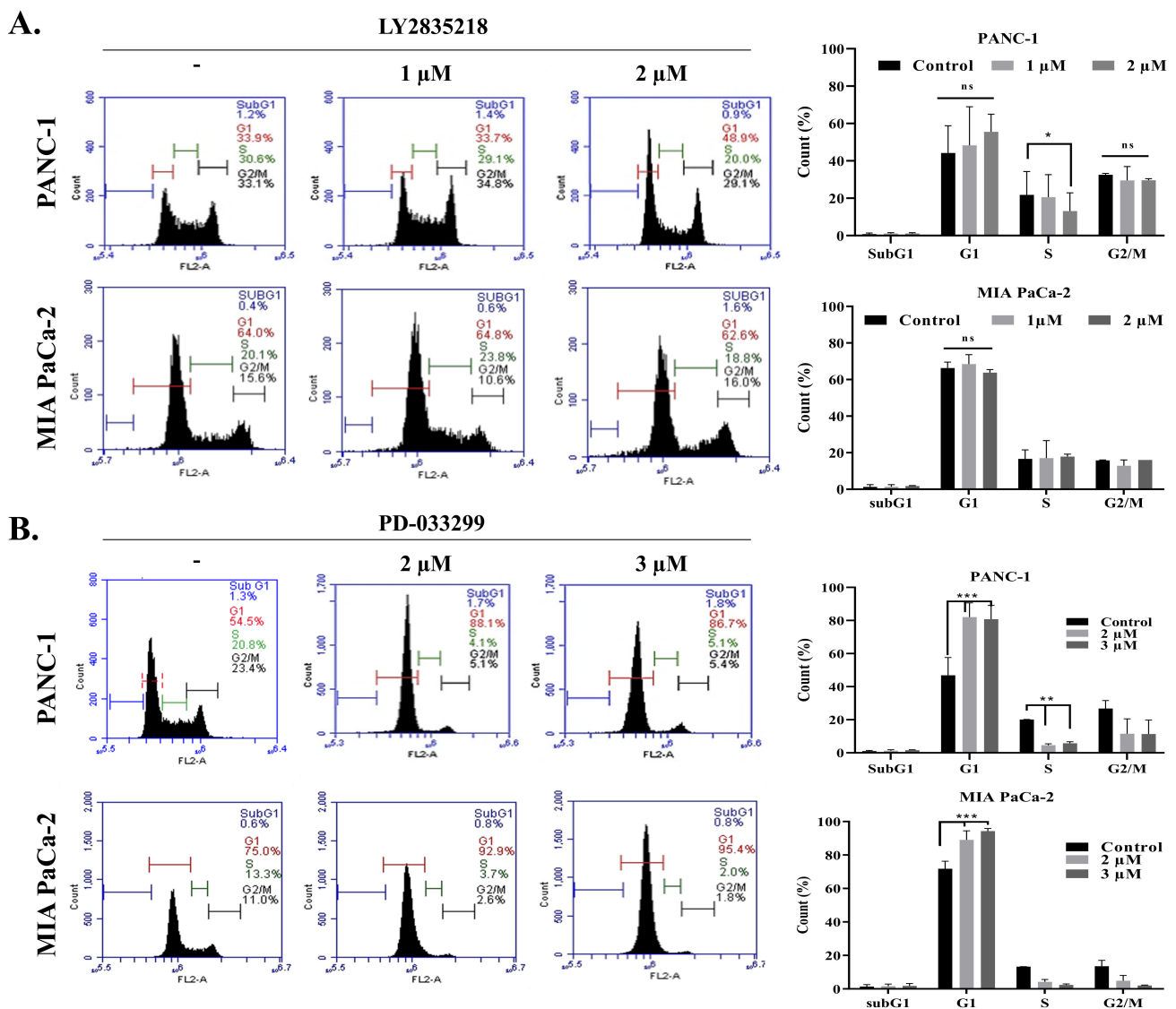


Figure 2. LY2835219 and PD-0332991 induced cell cycle arrest in PANC-1 and MIA PaCa-2 cells. Cells were treated with (A) LY2835219 (1–2 μ M) and (B) PD-0332991 (2 and 3 μ M) for 24 h. After drug treatment cells were fixed with 70% EtOH at +4 $^{\circ}$ C for a week and stained with PI. The cells were analyzed by flow cytometry (20,000 events/each condition). The histograms represented the mean \pm SD of with at least 2 separate experiments with two repeats * $p < 0.05$; ** $p < 0.01$; *** $p < 0.001$. After 2 and 3 μ M PD-0332991 treatments, no significant effect was observed in PANC-1 and MIA PaCa-2 cells at CDK4 protein expression levels (Figure 3D,E). The expression of CDK6 in the PANC-1 cell increased with 3 μ M PD-0332991 treatment and this effect was associated with an increased level of expression of cyclin D1 (Figure 3D). The p21 expression level increased by 2 and 3 μ M PD-0332991 treatment in both cell lines (Figure 3D,E). Interestingly we observed that Rb phosphorylation increased in the PANC-1 cell line as a result of PD-0332991 therapy (Figure 3D). Increasing doses of PD-0332991 treatment downregulated Rb phosphorylation in MIA PaCa-2 cell line (Figure 3E).

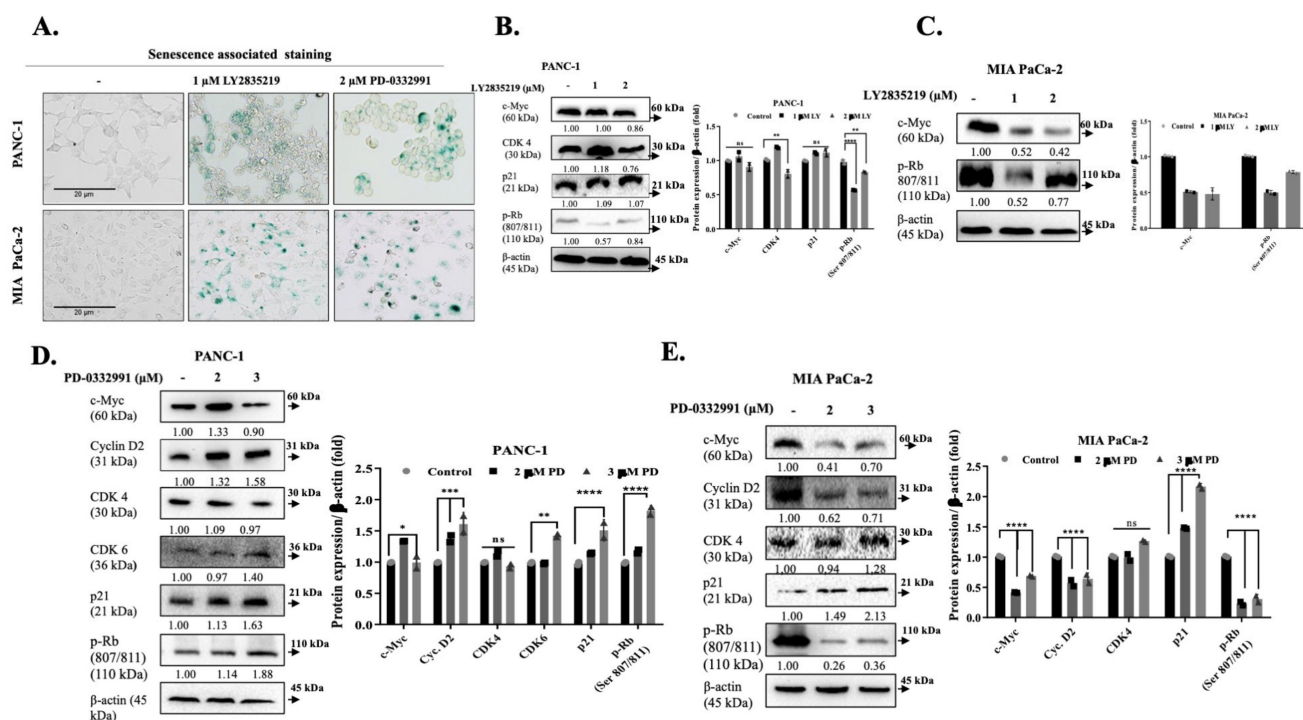


Figure 3. CDK4/6 inhibitors LY2835219 and PD-0332991 triggered cellular senescence in PANC-1 and MIA PaCa-2 cells. (A) Cells were exposed to Senescence β -Galactosidase Staining following treatment with each CDK inhibitor. After a night of Senescence β -Galactosidase staining, it was examined under a light microscope. Scale bar is 20 μ m. PANC-1 and MIA PaCa-2 cell lines treated with LY2835219 (B,C) and PD-0332991 (D,E) and the expression profile of the cell cycle signaling pathway proteins were determined by immunoblotting. (B) PANC-1 cells: c-Myc, CDK4, p21, and p-Rb (Ser807/811). (C) MIA PaCa-2 cells: c-Myc and p-Rb (Ser807/811). (D) PANC-1 cells: c-Myc, Cyclin D2, CDK4, CDK6, p21, and p-Rb (Ser807/811). (E) MIA PaCa-2 cells: c-Myc, Cyclin D2, CDK4, p21, and p-Rb (Ser807/811) β -actin was used as a loading control. The histograms show the average \pm SD according to the ImageJ analysis of the blots for each experiment ($n = 2$) * $p < 0.05$; ** $p < 0.01$; *** $p < 0.001$; **** $p < 0.0001$. 2.3. LY2835219 and PD-0332991 Are Fine-Tuning Agents to Prevent the Functional Role of the PI3K/AKT/mTOR Pathway via Modulating AMPK.

To understand the relationship between cell cycle arrest and the cellular senescence process, we performed an SA- β galactosidase test. We compared the cellular senescence processes after LY2835219 and PD-0332991 treatment in PANC-1 and MIA PaCa-2 cells compared to control cells (Figure 3A). We performed the treatments with selected doses of LY2835219 (1 μ M) and PD-0332991 (2 μ M) in this experiment. The resulting cells stained positively with SA- β Gal showed that senescence is triggered in both cell lines. Additionally, each cell line's morphology has become round, which was clearly observed in PANC-1 cells following treatment of each CDK inhibitor.

In accordance with these data, we determined that the cell cycle markers were affected by the LY2835219 and PD-0332991 treatments in a dose-dependent manner. Following LY2835219 treatment in the PANC-1 cell line, we observed a dose-related decrease in the expression level of c-Myc, which is a proto-oncogene. CDK4 expression level decreased by 2 μ M LY2835219 treatment. The level of Rb phosphorylation at Ser807/811, which means suppression of Rb and activation of cell cycle, decreased after 1 μ M and 2 μ M LY2835219 treatment in PANC-1. However, 1 μ M LY2835219 treatment further decreased the p-Rb (Ser 807/811) in PANC-1 cells (Figure 3B and Figure S1E,F). In the MIA PaCa-2 cell, we observed that the level of proto-oncogene c-Myc expression decreased with increasing doses, while the Rb phosphorylation decreased, especially with 1 μ M of LY2835219 treatment (Figure 3C and Figure S1A–D). A similar experiment was performed with PD-0332991 treatment and we observed that the level of c-Myc protein expression in the PANC-1 cell decreased with 3 μ M PD-0332991 (Figure 3D). Although this effect was regarded as a result of increasing

doses of palbociclib, 2 μM of the PD-0332991 treatment reduced the level of expression significantly in MIA PaCa-2 cells (Figure 3E). Interestingly, the cyclin-D2 expression level increased in the PANC-1 cell line, while increasing the dose of the PD-0332991 treatment decreased its expression in MIA PaCa-2 cells (Figure 3D,E).

The crosstalk between AMPK and the PI3K/Akt/mTOR pathway is an important process for the balance of cellular energy metabolism and coordination of cell proliferation. To investigate the therapeutic efficiency of LY2835219 and PD-0332991 on this pathway, we first examined the effect of LY2835219 in a dose-dependent manner for 24 h on the AMPK related PI3K/AKT/mTOR signaling pathways in PANC-1 and MIA PaCa-2 cells by immunoblotting. Increasing doses of LY2835219 treatment did not show any significant effect on PI3K p85 expression in PANC-1 cells. Interestingly, 1 μM LY2835219 upregulated the PI3K p85 but 2 μM LY2835219 had no significant effect in MIA PaCa-2 cells. The level of phosphorylated AKT (Ser473) expression in PI3K downstream molecules was investigated in the presence of LY2835219. Only LY2835219 at 2 μM was effective in reducing p-AKT (Ser453) in PANC-1 cells but decreased in a dose-dependent manner in MIA PaCa-2 cells. It is well known that the inhibition of GSK3 β is under the control of the AKT signaling axis, so GSK3 β was not inhibited through Ser9 phosphorylation, due to reduced p-AKT (Ser453) in PANC-1 and MIA PaCa-2 cells compared to the untreated control samples. Additionally, it is now clear that both mTOR and AMPK pathways regulate cellular homeostasis at multiple levels. Protein synthesis, metabolism, and mitochondrial function are likely to play a role in the regulatory effects of both mTOR and AMPK on cancer cells. Interestingly, LY2835219 caused the dephosphorylation and downregulation of AMPK in PANC-1 and MIA PaCa-2. It is thought that the increase in p70S6K levels in PANC-1 cells may be due to the decrease of p-AMPK (Thr172). Although LY2835219 treatment downregulated p-AMPK (Thr172) protein levels, decreased p-p70S6K levels were determined in MIA PaCa-2 cells. We concluded that LY2835219 was able to suppress PI3K/Akt pathway and prevented the activation of the translational pathway in MIA PaCa-2 cells but the effect of LY2835219 on the translational mechanism might be different in PANC-1 cells (Figure 4A,B; Figures S2A,B and S3A,B). The effect of both 2 and 3 μM PD-0332991 treatments on the cell survival axis was examined by immunoblotting. Although 2 and 3 μM PD-0332991 had cytotoxic effects and reduced cell viability by almost 50% on each pancreatic cancer cells, it was recorded that the 3 μM concentration was more effective on the downregulation of the PI3K/AKT/mTOR signaling than 2 μM PD-0332991. The dose-dependent PD-0332991 treatment for 24 h increased the PI3K expression level at 2 μM in PANC-1 cells however, 3 μM had no significant effect. In contrast, increasing doses of PD-0332991 significantly decreased PI3K expression levels in MIA PaCa-2 cells. The phosphorylation status of PTEN is known as a suppressing the mechanism of the PI3K/AKT pathway. We found that increasing doses of PD-0332991 treatment significantly upregulated PTEN expression in PANC-1 cells but led to slight upregulation in MIA PaCa-2 cells. Although p-PDK-1 at Ser241 residue expression levels were augmented in PANC-1 after 2 μM PD-0332991, the expression levels of p-AKT at Ser473 residue were reduced significantly in a dose-dependent manner. Concomitantly, p-PDK-1 was downregulated significantly following dose-dependent PD-0332991 treatment in MIA PaCa-2 cells. However, PD-0332991 treatment did not exhibit any significant effect on p-AKT at Ser473 residue. Interestingly, 3 μM PD-0332991 upregulated the p-GSK3 β (Ser9), whereas the opposite effect was observed with 2 μM PD-0332991 in PANC-1. Nevertheless, PD-0332991 was able to decrease p-GSK3 β (Ser9) expression levels dose-dependently in MIA PaCa-2 cells. 3 μM PD-0332991 treatment significantly upregulated p-AMPK (Thr172) expression in PANC-1 cells whereas 2 μM PD-0332991 led to slight upregulation in MIA PaCa-2 cells (Figure 4C,D; Figures S2C,D and S3E). Although PD-0332991 did not alter p-mTOR levels in PANC-1 cells, mTOR inhibition decreased p-p70S6K expression levels. There was a significant dose-dependent decrease in p-mTOR and p-p70S6K levels in relation to p-AMPK in MIA PaCa-2 cells. Decreasing the p-mTOR Ser2448/mTOR rate as a result of cell starvation provides a correlation with PD-0332991 treated cells with increased AMPK activity. We concluded that cell starvation is detected

metabolically by sensor mechanism on mTOR in LY2835219 treated cells. To confirm whether the induction of cell death was associated with the loss of the mitochondrial membrane potential, cells were stained by DiOC6 following treatment of the selected doses of LY2835219 (1 μ M) and PD-0332991 (2 μ M) for 24 h. The decrease of DiOC6-stained cells after drug treatment was observed by fluorescence microscopy and the relative intensity of DiOC6 staining was calculated and figured out in the graphic. It was consistent with MTT cell viability results which showed cell viability loss by almost 50% (Figure 4E).

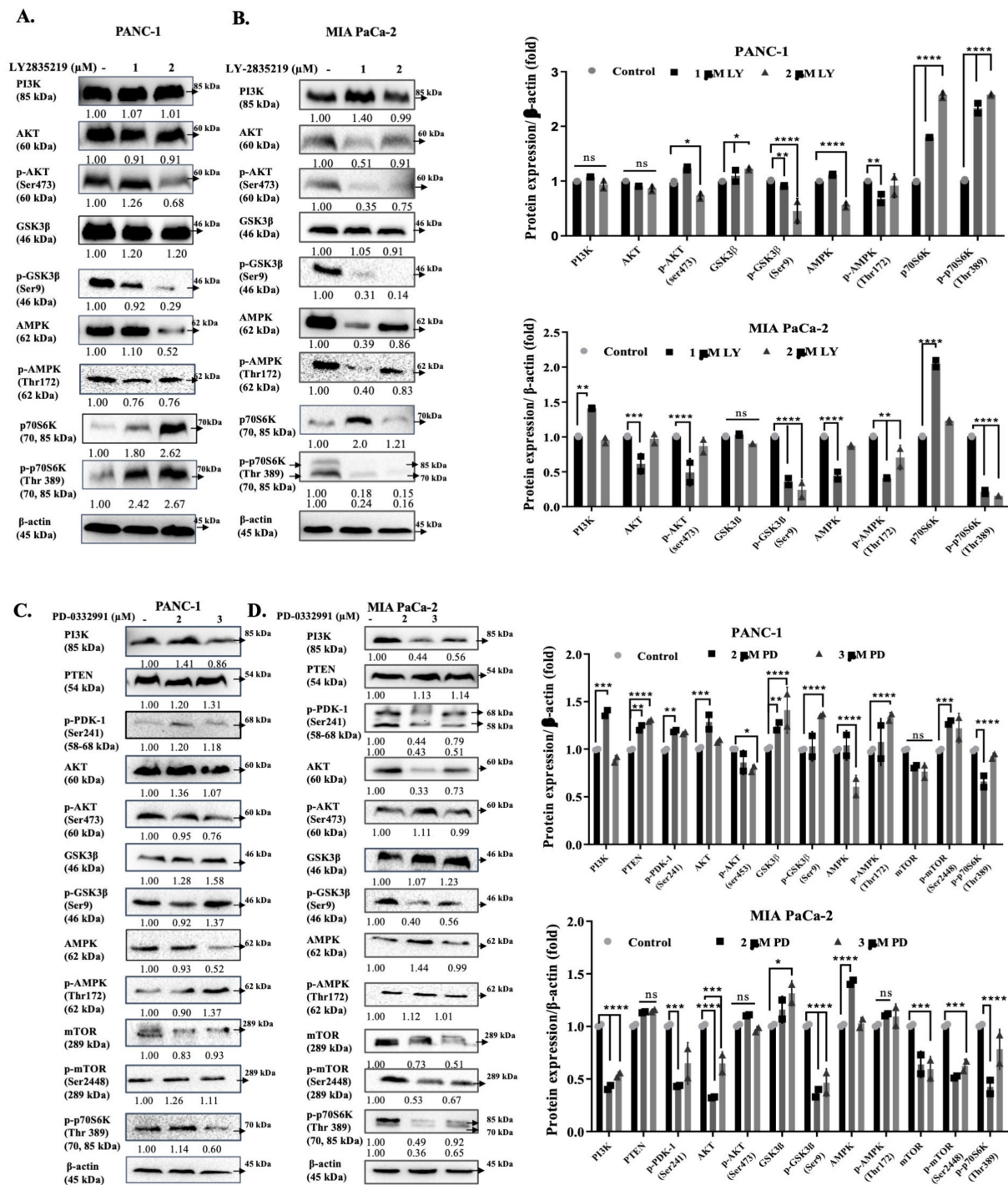


Figure 4. Cont.

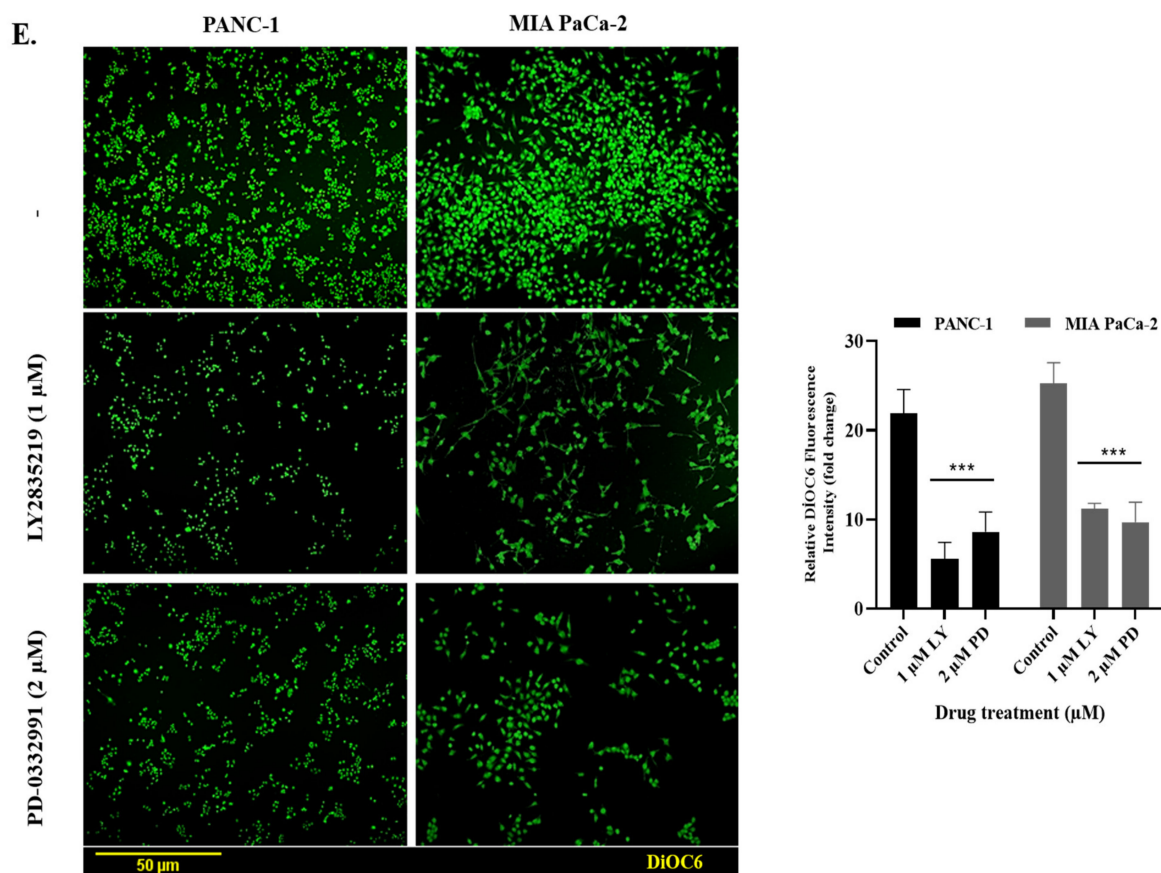


Figure 4. Effects of LY2835219 and PD-0332991 on the AMPK-related PI3K/AKT/mTOR signal axis. PANC-1 (A–C) and MIA PaCa-2 (B–D) cells were treated with LY2835219 (1–2 μM) and PD-0332991 (2–3 μM) for 24 h, and the expression profile of cell survival markers such as, PI3K p85, PTEN, p-PDK-1 (Ser241), AKT, p-AKT (Ser473), GSK3β, p-GSK3β (Ser9), AMPK, p-AMPK (Thr172), mTOR, p-mTOR (Ser2448), and p-p70S6K was analyzed by immunoblotting. β-actin was used as a loading control. The histograms represented the mean ± SD of 2 separate experiments. Data was evaluated by 2-way ANOVA analyzed by two-way ANOVA and Tukey’s multiple comparison test, $n = 2$, $p > 0.05$; * $p < 0.05$; ** $p < 0.01$; *** $p < 0.001$; **** $p < 0.0001$. (E) Mitochondrial membrane potential loss was examined by DiOC6 staining of PANC-1 and MIA PaCa-2 cells following treatment of the LY2835219 (1 μM) and PD-0332991 (2 μM). Scale bar is 50 μm. Stained cells were visualized by fluorescence microscopy (excitation = 485 nm, emission = 538 nm). The intensity of relative DiOC6 fluorescence was shown with the bar graph. Values are means ± SD, $n = 2$.

2.3. LY2835219 and PD-0332991 Induced Apoptosis in Time-Dependent Manner But the Cell Death Decision Was Taken at a Later Stage

The time-dependent effect of LY2835219 and PD-0332991 on apoptotic induction in MIA PaCa-2 and PANC-1 cells were examined with annexin V-PI staining. As shown in Figure 5A,B, PD-0332991 (2 μM) affected the total apoptotic cell death of PANC-1 in the lower left quadrant at 24 h as 10% ratio. We did not observe any apoptotic induction in PANC-1 for LY2835219 (1 μM) treatment. Similarly, LY2835219 (1 μM) and PD-0332991 (2 μM) did not significantly induce apoptosis in MIA PaCa-2 cells. The early apoptotic effect of LY2835219 (1 μM) and PD-0332991 (2 μM) were increased to 30% and 27% in PANC-1 cells within 48 h, respectively. Similarly, 20% of the early apoptotic MIA PaCa-2 cell population was determined following LY2835219 (1 μM) exposure. In contrast, we did not observe any apoptotic induction after PD-0332991 (2 μM) treatment for either 24 h or 48 h in MIA PaCa-2 cells. Both drugs did not lead to increased apoptotic cell population following 24 h treatment. Additionally, early apoptotic cells were observed following 48 h of treatment in PANC-1 cells but not in MIA PaCa-2 cells. Therefore, the increasing ratio of Annexin V-positive cells which means early apoptosis, was further investigated

by Caspase3/7 activation assay for 48 h of treatment. Caspase-3/7 activation is a critical process in apoptosis induction. Therefore, Caspase3/7 activity assay was performed in order to determine the apoptotic effects of 1 μM LY2835219 and 2 μM PD-0332991 treatment following 48 h of treatment in PANC-1, MIA PaCa-2 PDAC cell lines and normal non-tumorigenic HPDE cells, respectively. 1 μM LY2835219 more efficiently increased the caspase 3/7 activity in PANC-1 and HPDE cells more than MIA PaCa-2 cells. Therefore, it can be concluded that the early apoptotic effect of 1 μM LY2835219 in MIA PaCa-2 cell was in a Caspase 3/7 independent manner (Figure 5C). Moreover, 2 μM of PD-0332991 treatment for 48 h was efficient in all cell lines including HPDE cells.

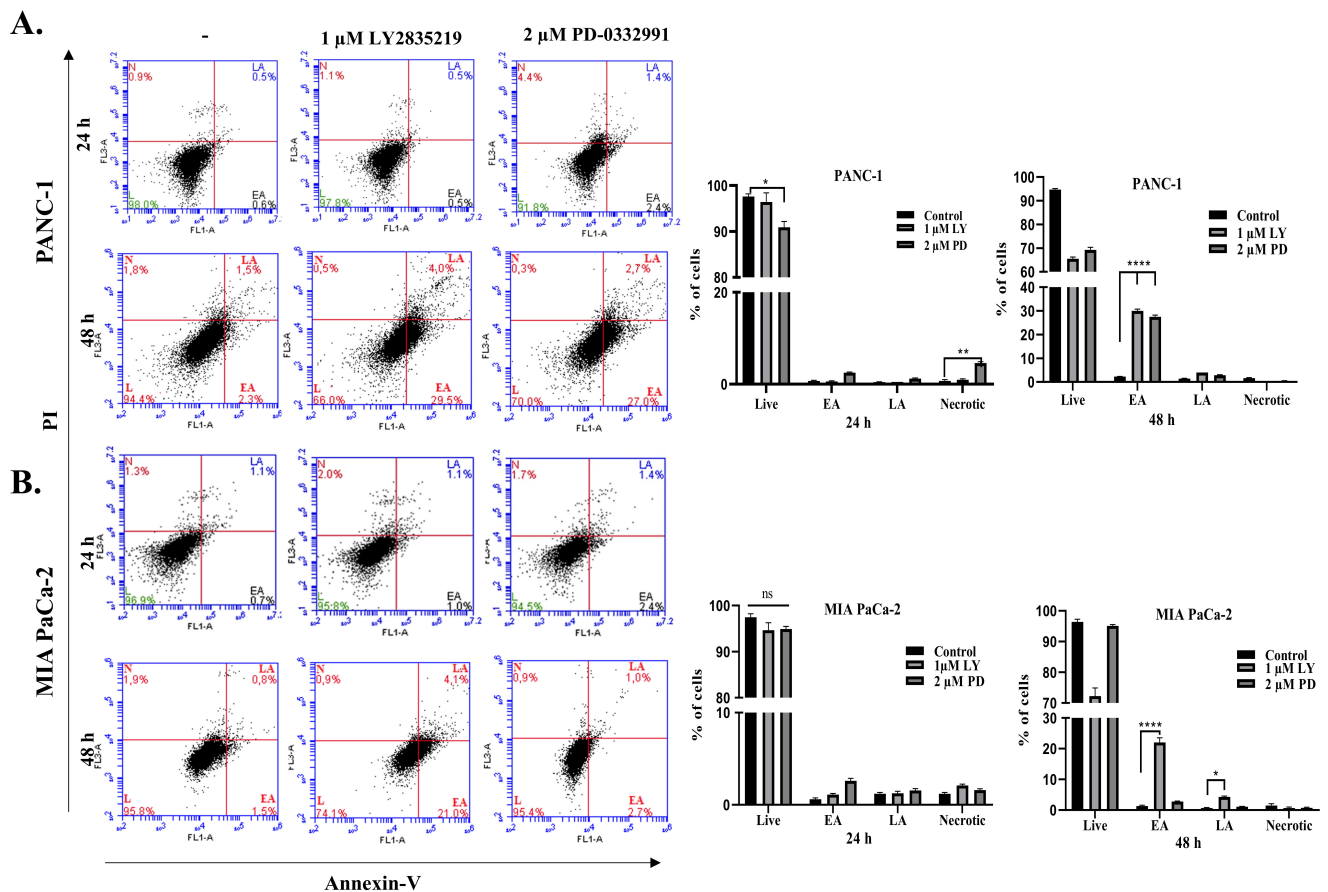


Figure 5. Cont.

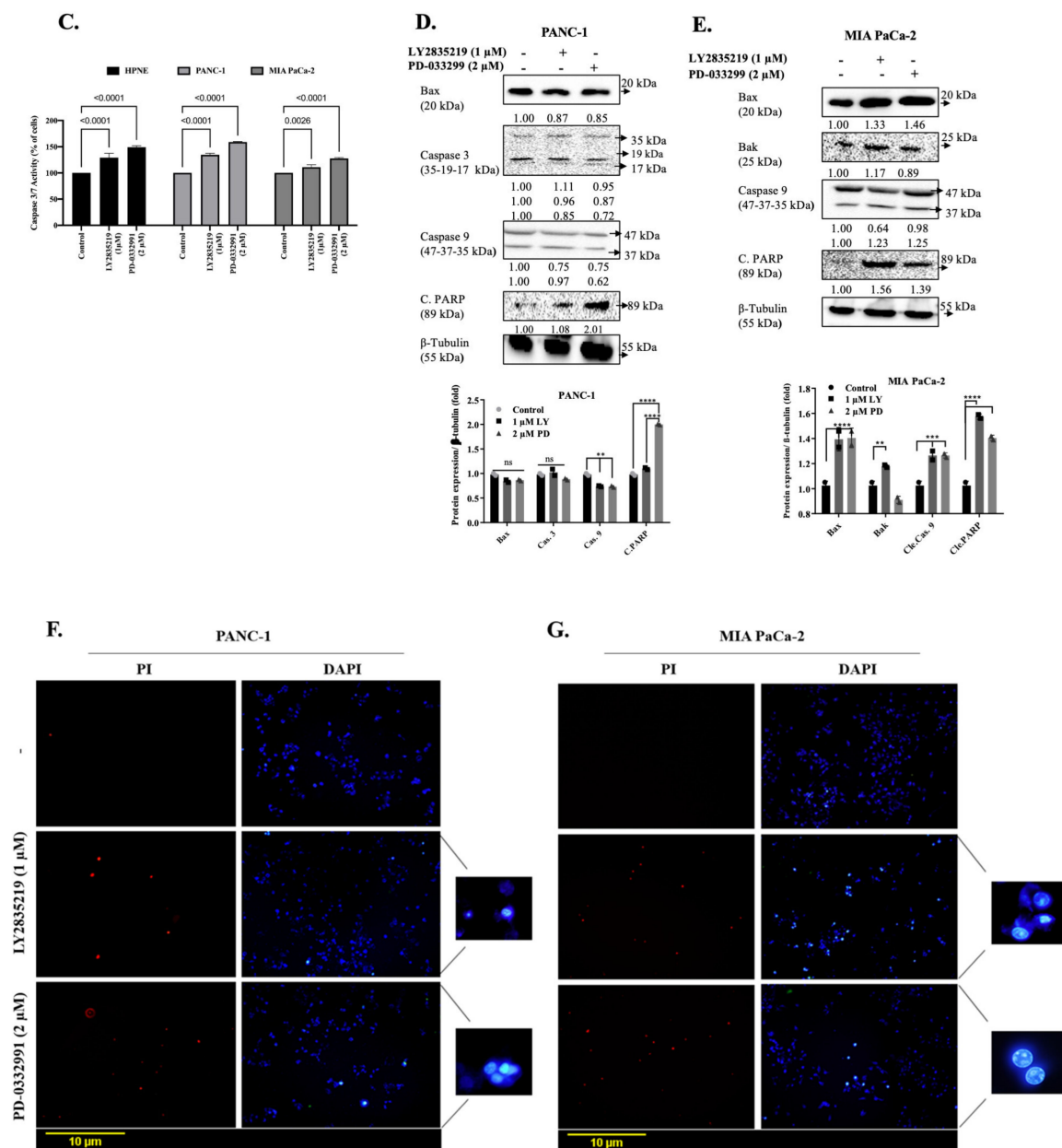


Figure 5. Effects of LY2835219 and PD-0332991 on apoptotic cell death. Apoptotic cell-death measured by Annexin-V/PI staining in (A) PANC-1 and (B) MIA PaCa-2 cells. Cells were treated with LY2835219 (1 μ M) and PD-0332991 (2 μ M) for 24 h and 48 h. Apoptosis was measured by Annexin-V/PI staining followed by flow cytometry. Data was evaluated by 2-way ANOVA analyzed by two-way ANOVA and Tukey's multiple comparison test $p > 0.05$; * $p < 0.05$; ** $p < 0.01$; *** $p < 0.001$; **** $p < 0.0001$. The histograms represented the mean \pm SD from two separate experiments with two repeats. (C) PANC-1, MIA PaCa-2 and HPDE cells were treated with LY2835219 (2 μ M) and PD-0332991 (2 μ M) for 24 h, and the caspase 3–7 activities were analyzed **** $p < 0.0001$. The histograms represented the mean \pm SD from two separate experiments with three repeats. (D) PANC-1 and (E) MIA PaCa-2 cells were treated with LY2835219 (1 μ M) and PD-0332991 (2 μ M) for 24 h, and the expression profile of apoptotic cells death markers such as Bax, Bak, caspase 9, caspase 3 and cleaved-PARP were analyzed by immunoblotting. β -tubulin was used as a loading control. The histograms show the average represents the mean \pm SD from two experiments. According to the ImageJ analysis of blots for each experiment. Data was evaluated by 2-way ANOVA analyzed by two-way ANOVA and Tukey's multiple comparison test $p > 0.05$; * $p < 0.05$; ** $p < 0.01$; *** $p < 0.001$; **** $p < 0.0001$. (F) PANC-1 and (G) MIA PaCa-2 cells were examined under a fluorescent microscope for $\times 100$ magnification. Scale bar is 10 μ m. Determination of cell death and DNA fragments induced by LY2835219 and PD-0332991. PI: excitation/emission (nm): 493/636 and DAPI: excitation/emission (nm): 358/461.

We checked the expression profile of apoptotic key proteins following LY2835219 and PD-0332991 in MIA PaCa-2 cells by immunoblotting. Although LY2835219 and PD-0332991 treatments did not significantly affect Bax expression in PANC-1 cells, each drug upregulated the Bax and Bak protein expression in MIA PaCa-2 cells. In PANC-1 cells, PD-0332991 (2 μ M) triggered significant PARP cleavage without showing any effect on caspase-9 and -3 activation. Cleaved PARP was increased in a similar way with caspase-9 activation after LY2835219 (1 μ M) and PD-0332991 (2 μ M) treatment in MIA PaCa-2 cells (Figure 5D,E and Figure S3C,D). We determined cell death following LY2835219 (1 μ M) and PD-0332991 (2 μ M) treatment in each cell line for 24 h shown by PI staining. Positive stained cells were accepted as dead, which were found increased following drug treatments. We also visualized nuclear condensation and DNA fragmentation due to the increased apoptosis with DAPI staining in the cells (Figure 5F,G).

We concluded that PD-0332991 was more effective than LY2835219 to trigger cell death within 24 h for PANC-1 cells. In addition, both LY2835219 and PD-0332991 did not induce apoptosis in MIA PaCa-2 cells for 24 h. Moreover, it was shown that due to the increasing senescence and cell cycle blocking process, the cell death decision was made at a later stage, however, it was active in the cell death order due to the change of the molecular markers of the cell.

3. Discussion

This study evaluated the AMPK signaling cascade, by assessing upstream and downstream targets, which was affected by the CDK4/6 inhibitors; LY2835219 and PD-0332991 in PANC-1 and MIA PaCa-2 PDAC cell lines. We confirmed that CDK4/6 inhibitors reduced cell viability significantly compared to untreated control cells [29,44]. However, more inhibitory effects on the MIA PaCa-2 compared to the PANC-1 cells were observed even though the cytotoxicity results were similar. Moreover, the long-term effects of LY2835219 and PD-0332991 showed that the PANC-1 cells were more sensitive than MIA PaCa-2 cells. This issue is common in other cell lines; Capan-2, PL5, Hs766t, and PL45 cell lines were found to be more sensitive against PD-0332991 (0.5, 1 and 2 μ M), colony formation of Capan-2 and PL45 cells were not altered following drug treatment [29,45].

Furthermore, the efficient chemotherapeutic potential of PD-0332991 was achieved at low doses and also with other therapeutic agents combined treatment. Moreover, the treatment with PD-0332991 at very low doses and in combination with enzalutamide increases the cytostatic effect and induces G1 arrest in triple-negative breast cancer [46]. It was shown that when the Huh7 and SNU398 hepatocarcinoma cell lines, either continuously or discontinuously, were exposed to PD-0332991, Huh7 cells, which showed an irreversible arrest at 0.1 μ M, were treated with a lower dose (68 nM) while SNU398 cells, which underwent a reversible cell cycle arrest at 0.5 μ M, were subjected to a higher dose (680 nM) [47]. Therefore, lower concentration alterations for CDK4/6 inhibitor treatment modalities may lead to diverse effects in cancer cells according to their genetic characteristics. Similarly, both LY2835219 and PD-0332991 decreased the cell viability and induced G1 arrest in PANC-1 and MIA PaCa-2 cells [48]. Our data also showed that treatment of PD-0332991 significantly triggered G1 arrest in both of the cells lines we used compared to LY2835219 exposure.

The expression of Rb, a cell cycle regulator, has been used to predict the drug resistance mechanism of cells. LY2835219 (1 μ M) exposure decreased the phosphorylated Rb protein levels in PANC-1 and MIA PaCa-2 cell lines. PD-0332991 treatment induced G1 arrest in MIA PaCa-2 and PANC-1 cell lines has been demonstrated in a similar trend with previous findings [44,45]. Moreover, PD-0332991 treatment leads to Rb hyperphosphorylation in the PANC-1 cell line and also, it is reported that a loss of Rb in cells can induce self-replication stress by leading to p16 accumulation. Studies have shown that higher expression levels of p16 led to resistant phenotype against CDK4/6 inhibition [49,50]. Although the deletion of the p16 copy number is seen in many cancer types, it has the potential to become ineffective as a result of DNA methylation [49]. The deletion of p16 causes sensitivity against

PD-0332991 treatment might be the cause of the effective response of MIA PaCa-2 cells against PD-0332991 exposure, and adverse effect in the PANC-1 cell line. In another study, when p16 silenced Rb remains dysfunctional as a regulator that allows uncontrolled proliferation [38,51]. Therefore, we thought that PD-0332991 triggered Rb hyperphosphorylation in the PANC-1 cell line showing aggressive properties and loss of p16. CDK4/6 activity in cells is upregulated in cancers by specific cyclin D amplification and various genomic changes in the cell, including natural CDK4/6 inhibitors such as CDKN2A [50,52].

These results also suggested whether the reason for the variability in cell cycle arrest dependent on the drug, dose, and cell line. The inducer roles of LY2835219 and PD-0332991 in PANC-1 and MIA PaCa-2 cell lines were examined in terms of senescence, and SA- β -Gal positive staining was observed in both cell lines, which triggered cellular senescence. However, in the PANC-1 cell line, a significant change was observed in cell morphology, especially as a result of the treatment of PD-0332991. The increased expression of p21, which is a cell cycle regulator protein, was recorded with the triggering of cellular senescence. In line with this result, we examined the expression level of target proteins involved in cell cycle [53]. Dose-dependent CDK4/6 inhibitors (LY2835219 and PD-0332991)-mediated p21 expression upregulation might be due to cellular senescence in PANC-1 cells. Also, a similar result was observed in the MIA PaCa-2 cell line with alone PD-0332991 treatment. While early triggering of the senescence process protects the cell against transformation, it has been stated that the long-term senescence process that occurs in cells triggers the development of cancer. Researchers have reported that the continuation of metabolic activity during cellular senescence can increase the expression may trigger tumor formation by expressing the inflammatory cytokines (IL-6 and IL-8), as well as chemokines that attract inflammatory cells and affect neighboring cells [54,55]. However, it has been shown that PD-0332991 treatment of AGS gastric cancer cells triggered the cellular senescence and affected the survival mechanisms in this way [56,57]. In PANC-1 cells, a decrease in CDK4 expression level, as well as an increase in p21 protein expression, was observed following PD-0332991 treatment and a dose-dependent downregulation in c-Myc were also determined after each CDK4/6 inhibitor treatment. In the H460 lung cancer cell line, as a result of LY2835219 (10 μ mol/L) treatment, it was observed that LY2835219 decreased Rb phosphorylation and increased p21 expression level [58]. No significant change was observed in CDK4 expression in MIA PaCa-2 cells due to the dose-dependent PD-0332991 (2 and 3 μ M) treatment. However, cyclin D1, which is an invigilator of CDK4, and c-Myc, which is involved in cell survival, resulted in a decrease in the expression level and Rb hypophosphorylation. Thereby, it caused a significant increase in the expression of one of the Cyclin-CDK inhibitors, p21, and has a significant effect on the molecular mechanism of cell cycle arrest and cellular senescence process. In PDAC cells, kinase assays from treated cells showed that the detectable CDK2 activity in PD-0332991 treated pancreatic cancer cells that retain the CDK2 protein and depleted CDK2 resulted in the potent suppression of RB phosphorylation.

PI3K/AKT/mTOR plays an essential role in controlling cell growth, proliferation, migration, and metabolism [18–20]. The downregulation of p-AKT and Raptor in PD-0332991-treated pancreatic cancer cells was consistent with our data [59]. The intracellular energy homeostasis or the anabolic activity of cells was associated with the PI3K/AKT/mTOR signaling axis [19,60]. Activation of upstream mitogenic pathways that increase CDK4/6 activity creates resistance to therapy in most tumor types [26,61]. More than 90% of PDAC tumors harbor driver mutations in K-Ras that activate various downstream signaling pathways such as the PI3K pathway [20,62,63]. The recent publications highlight the importance of PI3K signaling in stromal cells [20]. Therefore, PI3K/AKT/mTOR signaling has been focused as a key therapeutic target to hinder cell proliferation and then triggered apoptosis. This study investigated the molecular targets of LY2835219 and PD-0332991 related to PI3K/AKT/mTOR signaling axis in PANC-1 and MIA PaCa-2 cells. When the major changes were evaluated, interestingly, LY2835219 treatment in dose-dependent manner did not show any significant effect on PI3K levels in each cell line. Still, the expression level of

p-AKT (Ser473) was reduced by treatment of LY2835219 in PANC-1 (only at 2 μ M dose) and MIA PaCa-2 cells. The effect of dose-dependent PD-0332991 treatment decreased the PI3K and p-PDK-1 levels in MIA PaCa-2 cells. Although PI3K and p-PDK-1 levels were not affected by PD-0332991 treatment in PANC-1 cells, p-AKT at Ser473 was decreased and PTEN was increased by PD-0332991 treatment in both cell lines. The phosphorylation status of PTEN is known as a suppressing mechanism on the PI3K/AKT pathway [64]. The mouse PDAC is driven by oncogenic K-RAS mutation and PTEN deficiency also causes the spontaneous loss of Ink4a expression and shows pro-metastatic capacity [65]. Therapeutic potential of CDK4/6 inhibitors on aggressive cancer types were supported by results on combined treatment of PI3K and CDK4/6 inhibitors via cyclin D1 downregulation in HR+/HER2- breast cancer cells [19,66,67].

According to previous studies, AMPK, identified as a well-known regulator of cellular energy homeostasis, has been shown to cross-communicate via the PI3K/AKT/mTOR signaling axis [22–24]. AMPK activity can influence various effector proteins involved in different regulatory processes such as mTOR signaling that is associated with the pathogenesis of cancer [68]. Here, it was observed that both CDK4/6 inhibitors exerted various results on mTOR signaling. AMPK activation induced by CDK4/6 inhibitors enhances the therapeutic potential of these inhibitors through regulation of intracellular energy metabolism by controlling mTOR activity [68,69]. LY2835219 and PD-0332991 treatment decreased p-p70S6K levels in MIA PaCa-2 cells. However, the effect of LY2835219 on the translational mechanism might be different in PANC-1 cells. Besides, although PD-0332991 (only at 3 μ M dose) did not alter p-mTOR levels in PANC-1 cells, inhibition of mTOR decreased p-p70S6K levels. In our study, biological evidence from immunoblotting results showed that LY2835219 decreased the p-AMPK expression levels, which was higher in MIA PaCa-2 cells than PANC-1 cells. In contrast, PD-0332991 increased the p-AMPK at Thr172 residue in PANC-1 (only at 3 μ M dose) and MIA PaCa-2 (led to slight upregulation at 2 μ M dose). In a similar study, PD-0332991 induced p-AMPK (Thr172) levels, preventing tumor formation in PLC5 hepatocellular carcinoma cells [33]. In another study, AMPK activation loss has been shown to increase in PANC-1 and BxPC-3 PDAC cell lines invasion and metastasis through an HSF1-dependent [17]. Activation or inactivation of GSK-3 β is under control of the AKT and AMPK signaling axis. In addition, GSK-3 β plays a role in β -catenin-pathway dependent invasiveness in cancer cells [70]. In our study, LY2835219 and PD-0332991 treated down-regulated phosphorylation of GSK-3 β at Ser9 in MIA PaCa-2 cells. Although PD-0332991 (3 μ M) upregulated GSK-3 β at Ser9 levels, no significant effect on c-Myc levels was determined in PANC-1 cells. Previous studies also claimed that inhibition of CDK4/6 exerted various effects on PANC-1 and MIA PaCa-2 cells because each pancreatic cancer cells had different expression levels of PI3K and AKT [44,71]. Therefore, the colony formation potential was affected differently which MIA PaCa-2 cells were more resistant to PD-0332991 treatment.

Although both the CDK4/6 inhibitors restricted the cell survival in each pancreatic cancer cell, there was no significant increase on apoptotic cells in 24 h treatment. When LY2835219 (1 μ M) and PD-0332991 (2 μ M) treatment was prolonged to 48 h, PANC-1 and MIA PaCa-2 PDAC cells were increased in the early apoptotic phase. But there was no apoptotic induction after PD-0332991 (2 μ M) treatment for 48 h in MIA PaCa-2 cell. Similar to our findings, it was well established that the effect of CDK4/6 inhibitors at 48 h are an apoptotic agent for aggressive B-cell lymphoma cell lines [72]. Another study showed that LY2835219 (0.5–2 μ M) at 24 h induced late apoptosis with Annexin V/PI in breast cancer cells [73]. Although PD-0332991 (1–2 μ M) induced cell cycle arrest in liposarcoma cells, PD-0332991 (1–2 μ M) treatment at 24 h did not significantly induce apoptosis. The same study showed that increasing concentrations of PD-0332991 induced apoptosis [74]. In our study, CDK inhibitors induced caspase-dependent apoptosis via modulating Bax and Bak proteins in MIA PaCa-2 cells. In contrast, CDK inhibitors induce caspase-independent apoptosis in PANC-1 via only increasing cleavage of PARP. Recent studies indicated that the suppressive effects of PD-0332991 on cell growth in most cell lines were mild and weaker

than those of LY2835219. Besides, LY2835219 completely suppressed cell proliferation and markedly induced apoptosis [72]. Another study showed that LY2835219 induces atypical cell death in A549 lung carcinoma cell lines characterized by the formation of cytoplasmic vacuoles derived from lysosomes [75]. In our study, each CDK inhibitor triggered MMP loss in PANC-1 and MIA PaCa-2 cells. AMPK played a crucial role on the mitochondria biogenesis and protecting membrane potential via stimulating Peroxisome proliferator-activated receptor-gamma coactivator (PGC-1) and Nuclear Respiratory Factor 1/2 (NRF1/2) expression [76]. Therefore, the regulation of AMPK was important for the MMP loss during the treatment of CDK inhibitors in pancreatic cancer cells. It can be concluded that both LY2835219 and PD-0332991 significantly induced cell cycle arrest and senescence mechanism, but the singular treatment of each CDK inhibitor could not induce apoptosis in PANC-1 and MIA PaCa-2 PDAC cells. Our data also point to the increased expression levels of cleaved PARP, which was associated with CDK inhibitors-induced senescence mechanisms [77].

4. Materials and Methods

4.1. Cell Lines and Reagents

PANC-1 (CRL-1469) and MIA PaCa-2 (CRL-1420) were purchased from American Type Culture Collection (ATCC, Rockville, MD, USA). The cells were cultured in Dulbecco's modified Eagle's medium (DMEM; GIBCO-Life Technologies, Carlsbad, CA, USA) supplemented with 10% fetal bovine serum (Pan Biotech GmbH, Aidenbach, Germany) and 1% penicillin/streptomycin (GIBCO Invitrogen; Carlsbad, CA, USA) and incubated in 37 °C with 5% CO₂ (HeraCell 150i ThermoLab systems, Beverly, MA, USA). LY2835219 and PD-0332991 were purchased from Selleck Chemicals (Houston, TX, USA) and were dissolved in dimethyl sulfoxide (DMSO) at an initial stock concentration of 10 mM and stored as aliquots at −20 °C [44]. Human Pancreatic Duct Epithelial Cell Line (H6c7, HPDE) was provided by Prof Hemant Kocher from Barts Cancer Institute, Queen Mary, University of London. The cells were cultured in keratinocyte serum-free medium (GIBCO, Invitrogen Co.) supplemented with 0.1 mg/mL bovine pituitary extract (BPE GIBCO, Invitrogen Co.) and 5 ng/mL epidermal growth factor (EGF, GIBCO, Invitrogen Co.).

4.2. Cell Viability Assay

The effects of the CDK4/6 inhibitors LY2835219 and PD-0332991 on PDAC cell lines and normal non-tumorigenic human pancreatic ductal epithelial cells (HPDE) viabilities were determined by a colorimetric MTT (3-(4,5-dimethylthiazol-2-yl)-2,5-diphenyltetrazolium bromide) assay. The cells were seeded at a density of 1×10^4 cells per well in 96-well plates and treated with LY2835219 and PD-0332991 (0–10 μM) for 24 h. Then, 10 μL of MTT dye (5 mg/mL in PBS, Sigma; St. Louis, MO, USA) was added to the culture medium and incubated at 37 °C for 4 h. To solubilize the formazan crystals that were converted from MTT by the mitochondrial enzymes, 100 μL DMSO (Sigma; St. Louis, MO, USA) was added. The absorbance of the suspension at 570 nm was measured with a microplate reader (Bio-Rad, Hercules, CA, USA) [44].

4.3. Colony Formation Assay

The cells were seeded at a density of 3×10^3 cells/well in 6-well plates and dispersed evenly by shaking the dishes slightly, allowed to adhere for 24 h. After attachment, the cells were treated with increasing concentrations of LY2835219 (0–3 μM) or PD-0332991 (0–4 μM). After 24 h, drug-containing media were removed, and the cells were allowed to form colonies in complete media for 10 days. The colonies were fixed with a solution of acetic acid and methanol (1:3) for 5 min, the supernatant was removed. Later, the cells were stained with 0.5% crystal violet for 30 min. Finally, the dye was washed away with distilled water. The clones were counted under a light microscope [44,78].

4.4. Determination of Apoptotic Cell Death and Cell Survival by Fluorescent Microscopy and Caspase 3/7 Activity Assay

The cells were seeded at 2×10^4 into 12 well plates and treated with LY2835219 (1 μ M) and PD-0332991 (2 μ M) for 24 h. Then washed once with 1X PBS and stained with 4 nM 3,3'-dihexyloxacarbocyanine iodide (DiOC6; Calbiochem, La Jolla, CA, USA; 40 nM stock concentrations in DMSO) for 15 min in the dark. Changes in mitochondrial membrane potential (MMP) were observed by fluorescence microscopy (Ex/Em: 488/525 nm, Olympus IX70). The cells were similarly seeded (2×10^4 into 12 well plates), and were stained with Propidium iodide (PI; Applichem, Darmstadt, Germany; 50 mg/mL stock concentration in 1X PBS) and incubated at 37 °C for 30 min. The cells were washed once with 1X PBS and apoptotic cells were visualized by fluorescence microscopy (Ex/Em: 536/617 nm, Olympus IX70). In parallel, cells were stained with 5 mg/mL 4',6-diamidino-2-phenylindole (DAPI; Sigma, St, Louis, MO, USA) and incubated at 37 °C for 10 min. The cells were then washed once with 1X PBS, and nuclear condensation was visualized in a fluorescence microscope with 350 nm excitation and 470 nm emission (Olympus, IX70) [44,78]. APOCYTO Caspase-3 Colorimetric Assay Kit (MBL, Nagoya, Japan) was used for the detection of caspase-3/7 activity following the manufacturer's protocol. Cells were harvested after 24-h incubation LY2835219 (1 μ M) and PD-0332991 (2 μ M) for 24 h and subjected to caspase-3 activity detection.

4.5. Senescence β -Galactosidase Staining

PANC-1 and MIA PaCa-2 cell lines were seeded as 3×10^5 cells in 6-well plates and were treated with selected LY2835219 (1 μ M) doses PD-0332991 (2 μ M) for 24 h. After 24 h of drug exposure, the medium was removed, and the cells were washed 2 times with 1X PBS. Cells were fixed according to the protocol indicated by Senescence β -Galactosidase Staining Kit #9860 (CST, Danvers, MA, USA), then they were microscopically examined after β -gal administration [38,79].

4.6. Cell Cycle Analysis by Flow Cytometry

The cells were seeded at a density of 5×10^4 in 6-well plates and exposed to LY2835219 (1–2 μ M) and PD-0332991 (2–3 μ M) for 24 h. Following trypsinization, the cells were centrifuged at 2000 rpm for 5 min. The cells were then fixed with 70% ethanol and incubated at -20 °C until the analysis [44]. Later, the cells were stained with a PI/RNase staining buffer for 30 min and analyzed by a flow cytometer (BD Accuri Bioscience, Franklin Lakes, NJ, USA). For each measurement, 1×10^4 cells were analyzed and measured using C6 plus software (BD Accuri Bioscience, Franklin Lakes, NJ, USA).

4.7. Determination of Cell Death by Annexin V/PI Analysis

PANC-1 and MIA PaCa-2 cells were seeded into 100 mm Petri dishes 1×10^6 cells/well then incubated for cell attachment overnight. Then cells were treated with LY2835219 (1 μ M) and PD-0332991 (2 μ M) for 24 h. Following drug exposure, the cells were washed with 1X PBS, they were removed with trypsin and the cells were centrifuged at 500 g for 5 min. PBS was removed from the pellet. After the FITC Annexin V Apoptosis Detection Kit (# 556547, BD Pharmingen™) was applied according to the specified protocol, the samples were read and analyzed in cell flow cytometry [78].

4.8. Western Blot Analysis

The cells were seeded at a density of 5×10^5 cells in 60-mm or 100-mm dishes and treated with a selected dose of LY2835219 and PD-0332991 for 24 h [44]. Following drug treatment, cells were scraped with ice-cold 1X PBS and lysed on ice in a protein lysis solution M-PER Mammalian Protein Extraction Reagent (Thermo Scientific). After the lysis procedure at room temperature for 15 min, cell debris was removed by centrifugation for 15 min at 13 200 rpm. Protein concentration was determined by the Bradford protein analysis assay. Total protein lysate (35–50 μ g) was loaded and separated on a 10–12% SDS-PAGE and then

transferred onto polyvinylidene difluoride (PVDF) membranes (Roche, Indianapolis, IN, USA). The membranes were then blocked with 5% non-fat milk blocked membranes which are dissolved in 0.1% TBS-T (10 mM Tris-HCl and Tween 20) and incubated with appropriate primary antibodies and horseradish peroxidase (HRP)-conjugated secondary antibodies for overnight at 4 °C (CST, Danvers, MA, USA). Following the addition of enhanced chemiluminescence reagent. Used antibodies; p-Rb Ser 807/811 (D20B12) #8516 (1:1000), c-Myc (D84C12) #5605 (1:1000), CDK4 (D9G3E) #12790 (1:1000), CDK6 (D4S8S) #13331 (1:1000), p21 (12D1) #2947 (1:1000), Cyclin D2 (D52F9) #3741 (1:1000), PI3K p85 (19H8) #4257 (1:1000), AKT (C67E7) #4691 (1:1000), p-Akt Ser473 (D9E) #4060 (1:1000), p-PDK1 Ser241b (49H2) #3438 (1:1000), PTEN (138G6) #9559 (1:1000), AMPK (D5A2) #5831 (1:1000), p-AMPK Thr172 (40H9) #2535 (1:1000), GSK3 β (27C10) #9315 (1:1000), p-GSK3 β Ser9 #9336 (1:1000), mTOR (7C10) #2983 (1:1000), p-mTOR Ser2448 (D9C2) #5536 (1:1000), P70S6K (49D7) #2708 (1:1000), p-P70S6K T389 (108D2) #9234 (1:1000), Bax (D2E11) #5023 (1:1000), Bak (D4E4) #12105 (1:1000), caspase 9 (C9) #9508 (1:1000), caspase 3 #9662 (1:1000), cleaved PARP #5625 (1:1000), and β -actin (13E5) #5125 (1:1000); polyclonal anti-rabbit/mouse antibodies were purchased from Cell Signaling Technology (CST, Danvers, MA, USA). Each antibody was diluted in superblock T20 reagent from Thermo Scientific (Beverly, MA, USA) at 1:500–1:1000 concentrations. HRP-conjugated secondary anti-rabbit and anti-mouse antibodies were from CST (1:3000). Images were taken at different time points and analyzed using the Olympus Micro DP Manager Image Analysis program. They were presented with bar graphs using Graph Pad software (version 4.04).

4.9. Statistical Analysis

All the statistical analyses of the experiments were performed using GraphPad Prism version 8.0.1 (<https://www.graphpad.com/>, accessed on 20 February 2021). The MTT cell viability assay and annexin V/PI staining were repeated three times and statistically analyzed by using two-way ANOVA and Sidak's multiple comparison test. The densitometric calculation of three replicate immunoblotting images was performed using ImageJ (<https://imagej.net/Welcome>, accessed on 14 February 2021) and analyzed by two-way ANOVA and Tukey's multiple comparison test. Significance levels are represented as the following: ns, $p > 0.05$; * $p < 0.05$; ** $p < 0.01$; *** $p < 0.001$; **** $p < 0.0001$. Error bars represent the average \pm standard deviation values.

5. Conclusions

In conclusion, we confirmed that LY2835219, which has a similar structural property to PD-0332991, shows a remarkable therapeutic effect in particular on metabolic rearrangement, cell survival, and cell death (Figure 6). We found that, both LY2835219 and PD-0332991 are strong apoptotic and senescence inducers based on the regulation of PI3K/AKT/mTOR signaling pathway via modulating AMPK. Decreasing p-mTOR Ser2448/mTOR rate as a result of cell starvation provided correlation with PD-0332991-treated cells with increased AMPK activity, and we concluded that cell starvation was detected metabolically by sensor mechanism on mTOR in LY2835219-treated cells.

In future studies, it might be critical to question the levels of AMPK regulated by LY2835219 in PDAC cell lines in terms of cell survival and death decision. LY2835219 and PD-0332991 could be promising candidates for combined drug therapy in aggressive PDAC. More studies are needed to clarify whether LY2835219 regulates AMPK in PDAC cell lines which then leads either cell survival or cellular death. Both LY2835219 and PD-0332991 could be promising candidates for combined drug therapy for PDAC.

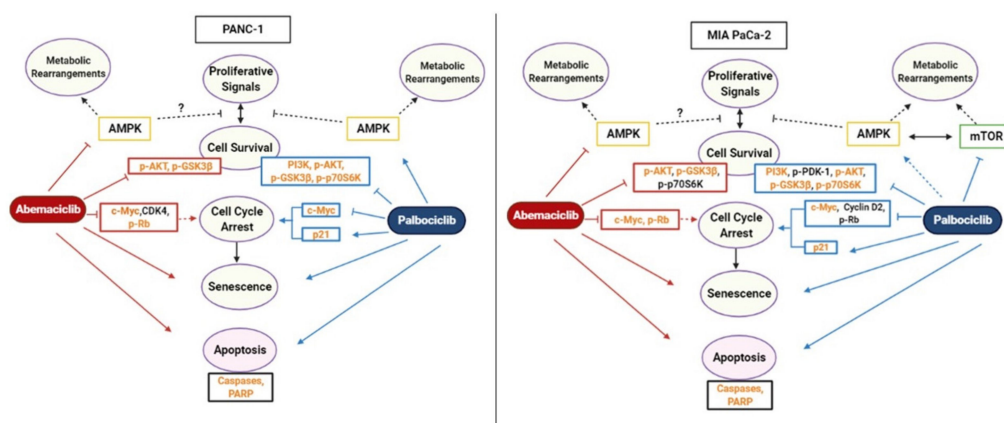


Figure 6. The schematic representation illustrates LY2835219 (Abemaciclib) and PD-0332991 (Palbociclib) effects in PANC-1 and MIA PaCa-2 cells. LY2835219 and PD-0332991 block the cell cycle to induce apoptosis or senescence. LY2835219 and PD-0332991 inhibit the PI3K/AKT pathway via modulating AMPK. Common molecular players are given in the orange color on the box to identify similarities between drugs and PDAC cell lines.

Supplementary Materials: The following are available online at <https://www.mdpi.com/2673-714/0/1/1/5/s1>, Figure S1: The results are presented as the result of second repeats from two separate biological replicates. Figure S2: The results of immunoblotting show representative the result of second repeats from two experiments according to the Image J analysis of blots. Figure S3: The results show that they represent the result of second replicates of two experiments.

Author Contributions: Conceptualization, E.D.A., P.O.-Y., A.C.-G. and P.U.O.; methodology, E.D.A., Ö.R., B.S. and M.N.C.; validation, B.S. and M.N.C.; formal analysis, B.S. and M.N.C.; investigation, B.S. and M.N.C.; resources, E.D.A., P.O.-Y., A.C.-G. and P.U.O.; data curation, B.S. and M.N.C.; writing—original draft preparation, B.S., M.N.C. and E.D.A.; writing—review and editing, E.D.A., P.O.-Y., A.C.-G. and P.U.O.; supervision, E.D.A.; funding acquisition, E.D.A. All authors have read and agreed to the published version of the manuscript.

Funding: This research was funded by TUBITAK, The Scientific and Technological Research Council of Turkey) 1001 program (Project no: 118Z100) and the APC was fully waived by the Journal.

Institutional Review Board Statement: Not applicable.

Informed Consent Statement: Not applicable.

Data Availability Statement: The data presented in this study are available on request from the corresponding author.

Acknowledgments: This study was supported by TUBITAK (The Scientific and Technological Research Council of Turkey) 1001 program (Project no: 118Z100).

Conflicts of Interest: The authors declare no conflict of interest.

References

- Mihaljevic, A.L.; Michalski, C.W.; Friess, H.; Kleeff, J. Molecular mechanism of pancreatic cancer—Understanding proliferation, invasion, and metastasis. *Langenbeck's Arch. Surg.* **2010**, *395*, 295–308. [[CrossRef](#)]
- Bray, F.; Ferlay, J.; Soerjomataram, I.; Siegel, R.L.; Torre, L.A.; Jemal, A. Global cancer statistics 2018: GLOBOCAN estimates of incidence and mortality worldwide for 36 cancers in 185 countries. *CA Cancer J. Clin.* **2018**, *68*, 394–424. [[CrossRef](#)]
- Gordon-Dseagu, V.L.; Devesa, S.S.; Goggins, M.; Stolzenberg-Solomon, R. Pancreatic cancer incidence trends: Evidence from the Surveillance, Epidemiology and End Results (SEER) population-based data. *Int. J. Epidemiol.* **2018**, *47*, 427–439. [[CrossRef](#)]
- Conway, J.R.; Herrmann, D.; Evans, T.J.; Morton, J.P.; Timpson, P. Combating pancreatic cancer with PI3K pathway inhibitors in the era of personalised medicine. *Gut* **2019**, *68*, 742–758. [[CrossRef](#)] [[PubMed](#)]
- Bryant, K.L.; Mancias, J.D.; Kimmelman, A.C.; Der, C.J. KRAS: Feeding pancreatic cancer proliferation. *Trends Biochem. Sci.* **2014**, *39*, 91–100. [[CrossRef](#)]
- Young, R.J.; Waldeck, K.; Martin, C.; Foo, J.H.; Cameron, D.P.; Kirby, L.; Do, H.; Mitchell, C.; Cullinane, C.; Liu, W.; et al. Loss of CDKN2A expression is a frequent event in primary invasive melanoma and correlates with sensitivity to the CDK4/6 inhibitor PD0332991 in melanoma cell lines. *Pigment. Cell Melanoma Res.* **2014**, *27*, 590–600. [[CrossRef](#)] [[PubMed](#)]

7. Foulkes, W.D.; Flanders, T.Y.; Pollock, P.M.; Haywardt, N.K.; Gene, C. The CDKN₂A (p16) Gene and Human Cancer. *Molecular Med.* **1997**, *3*, 5–20. [[CrossRef](#)]
8. Regel, I.; Kong, B.; Raulefs, S.; Erkan, M.; Michalski, C.W.; Hartel, M.; Kleeff, J. Energy metabolism and proliferation in pancreatic carcinogenesis. *Langenbeck's Arch. Surg.* **2012**, *397*, 507–512. [[CrossRef](#)]
9. Weissmueller, S.; Manchado, E.; Saborowski, M.; Morris, J.P.; Wagenblast, E.; Davis, C.A.; Moon, S.H.; Pfister, N.T.; Tschaharganeh, D.F.; Kitzing, T. Mutant p53 Drives Pancreatic Cancer Metastasis through Cell-Autonomous PDGF Receptor β Signaling. *Cell* **2014**, *157*, 382–394. [[CrossRef](#)]
10. Rivlin, N.; Brosh, R.; Oren, M.; Rotter, V. Mutations in the p53 tumor suppressor gene: Important milestones at the various steps of tumorigenesis. *Genes Cancer* **2011**, *2*, 466–474. [[CrossRef](#)] [[PubMed](#)]
11. Hardie, D.G.; Ross, F.A.; Hawley, S.A. AMPK: A nutrient and energy sensor that maintains energy homeostasis. *Nat. Rev. Mol. Cell Biol.* **2012**, *13*, 251–262. [[CrossRef](#)]
12. Shackelford, D.B.; Shaw, R.J. The LKB1-AMPK pathway: Metabolism and growth control in tumour suppression. *Nat. Rev. Cancer* **2009**, *9*, 563–575. [[CrossRef](#)]
13. Fajas, L.; Lopez-Mejia, I.C. CDK4, a new metabolic sensor that antagonizes AMPK. *Mol. Cell. Oncol.* **2018**, *5*, e1409862. [[CrossRef](#)]
14. Lopez-Mejia, I.C.; Lagarrigue, S.; Giral, A.; Martinez-Carreres, L.; Zanou, N.; Denechaud, P.D.; Castillo-Armengol, J.; Chavey, C.; Orpinell, M.; Delacuisine, B.; et al. CDK4 Phosphorylates AMPK α 2 to Inhibit Its Activity and Repress Fatty Acid Oxidation. *Mol. Cell* **2017**, *68*, 336–349.e6. [[CrossRef](#)] [[PubMed](#)]
15. Fogarty, S.; Hardie, D.G. Development of protein kinase activators: AMPK as a target in metabolic disorders and cancer. *Biochim. Biophys. Acta Proteins Proteom.* **2010**, *1804*, 581–591. [[CrossRef](#)]
16. Hardie, D.G.; Iwadate, Y.; Yumura, S. The AMP-activated protein kinase pathway—New players upstream and downstream. *J. Cell Sci.* **2004**, *117*, 5479–5487. [[CrossRef](#)]
17. Chen, K.; Qian, W.; Li, J.; Jiang, Z.; Cheng, L.; Yan, B.; Cao, J.; Sun, L.; Zhou, C.; Lei, M. Loss of AMPK activation promotes the invasion and metastasis of pancreatic cancer through an HSF1-dependent pathway. *Mol. Oncol.* **2017**, *11*, 1475–1492. [[CrossRef](#)]
18. Iriana, S.; Ahmed, S.; Gong, J.; Annamalai, A.A.; Tuli, R.; Hendifar, A.E. Targeting mTOR in pancreatic ductal adenocarcinoma. *Front. Oncol.* **2016**, *6*, 4–9. [[CrossRef](#)]
19. Cretella, D.; Ravelli, A.; Fumarola, C.; La Monica, S.; Digiaco, G.; Cavazzoni, A.; Alfieri, R.; Biondi, A.; Generali, D.; Bonelli, M.; et al. The anti-tumor efficacy of CDK4/6 inhibition is enhanced by the combination with PI3K/AKT/mTOR inhibitors through impairment of glucose metabolism in TNBC cells. *J. Exp. Clin. Cancer Res.* **2018**, *37*, 1–12. [[CrossRef](#)]
20. Murthy, D.; Attri, K.S.; Singh, P.K. Phosphoinositide 3-kinase signaling pathway in pancreatic ductal adenocarcinoma progression, pathogenesis, and therapeutics. *Front. Physiol.* **2018**, *9*, 1–18. [[CrossRef](#)]
21. Bondar, V.M.; Sweeney-Gotsch, B.; Andreeff, M.; Mills, G.B.; McConkey, D.J. Inhibition of the phosphatidylinositol 3'-kinase-AKT pathway induces apoptosis in pancreatic carcinoma cells in vitro and in vivo. *Mol. Cancer Ther.* **2002**, *1*, 989–997.
22. El-Masry, O.S.; Al-Sakkaf, K.; Brown, B.L.; Dobson, P.R. Differential crosstalk between the AMPK and PI3K/Akt pathways in breast cancer cells of differing genotypes: Leptin inhibits the effectiveness of AMPK activation. *Oncol. Rep.* **2015**, *34*, 1675–1680. [[CrossRef](#)] [[PubMed](#)]
23. Han, F.; Li, C.F.; Cai, Z.; Zhang, X.; Jin, G.; Zahang, W.N.; Xu, C.; Wang, C.-Y.; Morrow, J.; Zhang, S.; et al. The critical role of AMPK in driving Akt activation under stress, tumorigenesis and drug resistance. *Nat. Commun.* **2018**, *9*, 4728. [[CrossRef](#)] [[PubMed](#)]
24. Tao, R.; Gong, J.; Luo, X.; Zang, M.; Guo, W.; Wen, R.; Luo, Z. AMPK exerts dual regulatory effects on the PI3K pathway. *J. Mol. Signal.* **2010**, *5*, 1. [[CrossRef](#)] [[PubMed](#)]
25. Feng, W.W.; Kurokawa, M. Lipid metabolic reprogramming as an emerging mechanism of resistance to kinase inhibitors in breast cancer. *Cancer Drug Resist.* **2019**, *3*, 1–17. [[CrossRef](#)] [[PubMed](#)]
26. Niu, Y.; Xu, J.; Sun, T. Cyclin-dependent kinases 4/6 inhibitors in breast cancer: Current status, resistance, and combination strategies. *J. Cancer* **2019**, *10*, 5504–5517. [[CrossRef](#)] [[PubMed](#)]
27. Jingwen, B.; Yaochen, L.; Guojun, Z. Cell cycle regulation and anticancer drug discovery. *Cancer Biol. Med.* **2017**, *14*, 348–362. [[CrossRef](#)]
28. Eggersmann, T.K.; Degenhardt, T.; Gluz, O.; Wuerstlein, R.; Harbeck, N. CDK4/6 Inhibitors Expand the Therapeutic Options in Breast Cancer: Palbociclib, Ribociclib and Abemaciclib. *BioDrugs* **2019**, *33*, 125–135. [[CrossRef](#)] [[PubMed](#)]
29. Franco, J.; Witkiewicz, A.K.; Knudsen, E.S. CDK4/6 inhibitors have potent activity in combination with pathway selective therapeutic agents in models of pancreatic cancer. *Oncotarget* **2014**, *5*, 6512–6525. [[CrossRef](#)]
30. Goel, S.; DeCristo, M.J.; McAllister, S.S.; Zhao, J.J. CDK4/6 Inhibition in Cancer: Beyond Cell Cycle Arrest. *Trends Cell Biol.* **2018**, *28*, 911–925. [[CrossRef](#)]
31. Marra, A.; Curigliano, G. Are all cyclin-dependent kinases 4/6 inhibitors created equal? *NPJ Breast Cancer* **2019**, *5*, 1–9. [[CrossRef](#)]
32. Frederick, M.O.; Lowery, C.D.; Shackelford, T.; Renschler, M.; Stephens, J.; Flack, R.; Blosser, W.; Gupta, S.; Stewart, J.; Webster, Y.; et al. Abemaciclib is Active in Preclinical Models of Ewing's Sarcoma via Multi-pronged Regulation of Cell Cycle, DNA Methylation, and Interferon Pathway Signaling. *Clin. Cancer Res.* **2018**, *12*, 151–161. [[CrossRef](#)]
33. Hsieh, F.S.; Chen, Y.L.; Hung, M.H.; Chu, P.Y.; Tsai, M.H.; Chen, L.J.; Hsiao, Y.J.; Shih, C.T.; Chang, M.J.; Chao, T.I.; et al. Palbociclib induces activation of AMPK and inhibits hepatocellular carcinoma in a CDK4/6-independent manner. *Mol. Oncol.* **2017**, *11*, 1035–1049. [[CrossRef](#)] [[PubMed](#)]

34. Zhan, J.; Wang, Y.; Li, S.; Wang, Y.; Tan, P.; He, J.; Chen, Y.; Deng, H.; Huang, W.; Lin, X.; et al. AMPK/TSC2/mTOR pathway regulates replicative senescence of human vascular smooth muscle cells. *Exp. Ther. Med.* **2018**, *16*, 4853–4858. [[CrossRef](#)] [[PubMed](#)]
35. Ding, L.; Cao, J.; Lin, W.; Chen, H.; Xiong, X.; Ao, H.; Yu, M.; Lin, J. The roles of cyclin-dependent kinases in cell-cycle progression and therapeutic strategies in human breast cancer. *Int. J. Mol. Sci.* **2020**, *21*, 1960. [[CrossRef](#)]
36. Law, M.E.; Corsino, P.E.; Narayan, S.; Law, B.K. Cyclin-dependent kinase inhibitors as anticancer therapeutics. *Mol. Pharmacol.* **2015**, *88*, 846–852. [[CrossRef](#)]
37. Musgrove, E.A.; Caldon, C.E.; Barraclough, J.; Stone, A.; Sutherland, R.L. Cyclin D as a therapeutic target in cancer. *Nat. Rev. Cancer* **2011**, *11*, 558–572. [[CrossRef](#)] [[PubMed](#)]
38. Dhir, T.; Schultz, C.W.; Jain, A.; Brown, S.Z.; Haber, A.; Goetz, A.; Xi, C.; Su, G.H.; Xu, L.; Posey, J., 3rd; et al. Abemaciclib is effective against pancreatic cancer cells and synergizes with HuR and YAP1 inhibition. *Mol. Cancer Res.* **2019**, *17*, 2029–2041. [[CrossRef](#)]
39. Bonelli, M.; La Monica, S.; Fumarola, C.; Alfieri, R. Multiple effects of CDK4/6 inhibition in cancer: From cell cycle arrest to immunomodulation. *Biochem. Pharmacol.* **2019**, *170*, 113676. [[CrossRef](#)] [[PubMed](#)]
40. Skowron, M.A.; Vermeulen, M.; Winkelhausen, A.; Becker, T.K.; Bremmer, F.; Petzsch, P.; Schönberger, S.; Calaminus, G.; Köhrer, K.; Albers, P.; et al. CDK4/6 inhibition presents as a therapeutic option for paediatric and adult germ cell tumours and induces cell cycle arrest and apoptosis via canonical and non-canonical mechanisms. *Br. J. Cancer* **2020**, *123*, 378–391. [[CrossRef](#)] [[PubMed](#)]
41. Shao, C.; Tu, C.; Cheng, X.; Xu, Z.; Wang, X.; Shen, J.; Chai, K.; Chen, W. Inflammatory and Senescent Phenotype of Pancreatic Stellate Cells Induced by Sqstm1 Downregulation Facilitates Pancreatic Cancer Progression. *Int. J. Biol. Sci.* **2019**, *15*, 1020–1029. [[CrossRef](#)]
42. Nardella, C.; Clohessy, J.G.; Alimonti, A.; Pandolfi, P.P. Pro-senescence therapy for cancer treatment. *Nat. Rev. Cancer* **2011**, *24*, 503–511. [[CrossRef](#)]
43. Duong, H.Q.; Hwang, J.S.; Kim, H.J.; Seong, Y.S.; Bae, I. BML-275, an AMPK inhibitor, induces DNA damage, G2/M arrest and apoptosis in human pancreatic cancer cells. *Int. J. Oncol.* **2012**, *41*, 2227–2236. [[CrossRef](#)]
44. Rencuzogullari, O.; Yerlikaya, P.O.; Gürkan, A.Ç.; Arisan, E.D.; Telci, D. Palbociclib, a selective CDK4/6 inhibitor, restricts cell survival and epithelial-mesenchymal transition in Panc-1 and MiaPaCa-2 pancreatic cancer cells. *J. Cell. Biochem.* **2020**, *121*, 508–523. [[CrossRef](#)]
45. Zhang, J.; Zhou, L.; Zhao, S.; Dicker, D.T.; El-Deiry, W.S. The CDK4/6 inhibitor palbociclib synergizes with irinotecan to promote colorectal cancer cell death under hypoxia. *Cell Cycle* **2017**, *16*, 1193–1200. [[CrossRef](#)]
46. Liu, C.Y.; Lau, K.Y.; Hsu, C.C.; Chen, L.J.; Lee, C.H.; Huang, T.T.; Chen, Y.T.; Huang, C.T.; Lin, P.H.; Tseng, L.M. Combination of palbociclib with enzalutamide shows in vitro activity in RB proficient and androgen receptor positive triple negative breast cancer cells. *PLoS ONE* **2017**. [[CrossRef](#)]
47. Bollard, J.; Miguela, V.; De Galarreta, M.R.; Venkatesh, A.; Bian, C.B.; Roberto, M.P.; Tovar, V.; Sia, D.; Molina-Sánchez, P.; Nguyen, C.B.; et al. Palbociclib (PD-0332991), a selective CDK4/6 inhibitor, restricts tumour growth in preclinical models of hepatocellular carcinoma. *Gut* **2016**, *66*, 1286–1296. [[CrossRef](#)]
48. Clark, A.S.; Karasic, T.B.; DeMichele, A.; Vaughn, D.J.; O'Hara, M.; Perini, R.; Zhang, P.; Lal, P.; Feldman, M.; O'Dwyer, P.J. Palbociclib (PD0332991)—A selective and potent cyclin-dependent kinase inhibitor: A review of pharmacodynamics and clinical development. *JAMA Oncol.* **2016**, *2*, 253–260. [[CrossRef](#)]
49. Li, P.; Zhang, X.; Gu, L.; Zhou, J.; Deng, D. P16 methylation increases the sensitivity of cancer cells to the CDK4/6 inhibitor palbociclib. *PLoS ONE* **2019**, *14*. [[CrossRef](#)]
50. García-Reyes, B.; Kretz, A.L.; Ruff, J.P.; von Karstedt, S.; Hillenbrand, A.; Knippschild, U.; Henne-Bruns, D.; Lemke, J. The emerging role of cyclin-dependent kinases (CDKs) in pancreatic ductal adenocarcinoma. *Int. J. Mol. Sci.* **2018**, *19*, 3219. [[CrossRef](#)]
51. Kim, E.S.; Kelly, K.; Paz-Ares, L.G.; Garrido, P.; Jalal, S.; Mahadevan, D.; Gutierrez, M.; Provencio, M.; Schaefer, E.; Shaheen, M.; et al. Abemaciclib in Combination with Single-Agent Options in Patients with Stage IV Non-Small Cell Lung Cancer: A Phase Ib Study. *Clin. Cancer Res.* **2018**, *24*, 5543–5551. [[CrossRef](#)]
52. Hamilton, E.; Infante, J.R. Targeting CDK4/6 in patients with cancer. *Cancer Treat. Rev.* **2016**, *45*, 129–138. [[CrossRef](#)]
53. Modrak, D.E.; Leon, E.; Goldenberg, D.M.; Gold, D.V. Ceramide regulates gemcitabine-induced senescence and apoptosis in human pancreatic cancer cell lines. *Mol. Cancer Res.* **2009**, *7*, 890–896. [[CrossRef](#)] [[PubMed](#)]
54. Campisi, J. Senescence, cellular senescence, and cancer. *Ann. Rev. Physiol.* **2013**, *75*, 685–705. [[CrossRef](#)]
55. Collado, M.; Blasco, M.A.; Serrano, M. Cellular Senescence in Cancer and Senescence. *Cell* **2007**, *130*, 223–233. [[CrossRef](#)] [[PubMed](#)]
56. Valenzuela, C.A.; Vargas, L.; Martinez, V.; Bravo, S.; Brown, N.E. Palbociclib-induced autophagy and senescence in gastric cancer cells. *Exp. Cell Res.* **2017**, *360*, 390–396. [[CrossRef](#)]
57. Franco, J.; Balaji, U.; Freinkman, E.; Witkiewicz, A.K.; Knudsen, E.S. Metabolic Reprogramming of Pancreatic Cancer Mediated by CDK4/6 Inhibition Elicits Unique Vulnerabilities. *Cell Rep.* **2016**, *14*, 979–990. [[CrossRef](#)] [[PubMed](#)]
58. Naz, S.; Sowers, A.; Choudri, R.; Wissler, M.; Gamson, J.; Mathias, A.; Cook, J.A.; Mitchell, J.B. Abemaciclib, a selective CDK4/6 inhibitor, enhances the radiosensitivity of non-small cell lung cancer in vitro and in vivo. *Clin. Cancer Res.* **2018**, *24*, 3994–4005. [[CrossRef](#)] [[PubMed](#)]

59. Knudsen, E.S.; Kumarasamy, V.; Ruiz, A.; Sivinski, J.; Chung, S.; Grant, A.; Vail, P.; Chauhan, S.S.; Jie, T.; Riall, T.S.; et al. Cell cycle plasticity driven by MTOR signaling: Integral resistance to CDK4/6 inhibition in patient-derived models of pancreatic cancer. *Oncogene* **2019**, *38*, 3355–3370. [[CrossRef](#)]
60. Hay, N. Interplay between FOXO, TOR, and Akt. *Biochim. Biophys. Acta BBA Bioenerg.* **2011**, *1813*, 1965–1970. [[CrossRef](#)]
61. McCartney, A.; Migliaccio, I.; Bonechi, M.; Biagioni, C.; Romagnoli, D.; De Luca, F.; Galardi, F.; Risi, E.; De Santo, I.; Benelli, M.; et al. Mechanisms of Resistance to CDK4/6 Inhibitors: Potential Implications and Biomarkers for Clinical Practice. *Front. Oncol.* **2019**, *9*, 2–9. [[CrossRef](#)]
62. Perugini, R.A.; McDade, T.P.; Vittimberga, F.J.; Callery, M.P. Pancreatic cancer cell proliferation phosphatidylinositol 3-kinase dependent. *J. Surg. Res.* **2000**, *90*, 39–44. [[CrossRef](#)]
63. Orgován, Z.; Keserű, G.M. Small molecule inhibitors of RAS proteins with oncogenic mutations. *Cancer Metastasis Rev.* **2020**, *39*, 1107–1126. [[CrossRef](#)]
64. Georgescu, M.-M. PTEN Tumor Suppressor Network in PI3K-Akt Pathway Control. *Genes Cancer* **2010**, *1*, 1170–1177. [[CrossRef](#)] [[PubMed](#)]
65. Kutlu, H.Y.; Elpek, G.; Stephanie, A.V.; Zimmerman, M.; Gerald, C.; Chu, H.Y.; Fletcher-Sananikone, E.; Zhang, H.; Liu, Y.; Wang, W.; et al. Pten a major tumor suppressor in PDAC. *Cancer Discov.* **2011**, *1*, 158–169. [[CrossRef](#)]
66. Michaloglou, C.; Crafter, C.; Siersbaek, R.; Delpuech, O.; Curwen, J.O.; Carnevalli, L.S.; Staniszewska, A.D.; Polanska, U.M.; Cheraghchi-Bashi, A.; Lawson, M.; et al. Combined inhibition of mtor and CDK4/6 is required for optimal blockade of e2f function and long-term growth inhibition in estrogen receptors—Positive breast cancer. *Mol. Cancer Ther.* **2018**, *17*, 908–920. [[CrossRef](#)]
67. Litchfield, L.M.; Boehnke, K.; Brahmachary, M.; Mur, C.; Bi, C.; Stephens, J.R.; Sauder, J.M.; Gutiérrez, S.M.; McNulty, A.M.; Ye, X.S.; et al. Combined inhibition of PIM and CDK4/6 suppresses both mTOR signaling and Rb phosphorylation and potentiates PI3K inhibition in cancer cells. *Oncotarget* **2020**, *11*, 1478–1492. [[CrossRef](#)]
68. Kang, J.I.; Hong, J.Y.; Lee, H.J.; Bae, S.Y.; Jung, C.; Park, H.J.; Lee, S.K. Anti-Tumor Activity of Yuanhuacine by Regulating AMPK/mTOR Signaling Pathway and Actin Cytoskeleton Organization in Non-Small Cell Lung Cancer Cells. *PLoS ONE* **2015**, *10*, e0144368. [[CrossRef](#)]
69. Romero-Pozuelo, J.; Figlia, G.; Kaya, O.; Martin-Villalba, A.; Teleman, A.A. Cdk4 and Cdk6 Couple the Cell-Cycle Machinery to Cell Growth via mTORC1. *Cell Rep.* **2020**, *31*, 107504. [[CrossRef](#)] [[PubMed](#)]
70. Huang, J.; Guo, X.; Li, W.; Zhang, H. Activation of Wnt/ β -catenin signalling via GSK3 inhibitors direct differentiation of human adipose stem cells into functional hepatocytes. *Sci. Rep.* **2017**, *7*, 1–12. [[CrossRef](#)]
71. Korur, S.; Huber, R.M.; Sivasankaran, B.; Petrich, M.; Jr, P.M.; Hemmings, B.A.; Merlo, A.; Lino, M.M. GSK3 β Regulates Differentiation and Growth Arrest in Glioblastoma. *PLoS ONE* **2009**, *4*, e7443. [[CrossRef](#)]
72. Tanaka, Y.; Momose, S.; Tabayashi, T.; Sawada, K.; Yamashita, T.; Higashi, M.; Sagawa, M.; Tokuhira, M.; Rosenwald, A.; Kizaki, M.; et al. Abemaciclib, a CDK4/6 inhibitor, exerts preclinical activity against aggressive germinal center-derived B-cell lymphomas. *Cancer Sci.* **2020**, *111*, 749–759. [[CrossRef](#)]
73. Torres-Guzmán, R.; Calsina, B.; Hermoso, A.; Baquero, C.; Alvarez, B.; Amat, J.; McNulty, A.M.; Gong, X.; Boehnke, K.; Du, J.; et al. Preclinical characterization of abemaciclib in hormone receptor positive breast cancer. *Oncotarget* **2017**, *8*, 69493–69507. [[CrossRef](#)]
74. Laroche-Clary, A.; Chaire, V.; Algeo, M.P.; Derieppe, M.A.; Loarer, F.L.; Italiano, A. Combined targeting of MDM2 and CDK4 is synergistic in dedifferentiated liposarcomas. *J. Hematol. Oncol.* **2017**, *10*, 123. [[CrossRef](#)]
75. Hino, H.; Iriyama, N.; Kokuba, H.; Kazama, H.; Moriya, S.; Takano, N.; Hiramoto, M.; Aizawa, S.; Miyazawa, K. Abemaciclib induces atypical cell death in cancer cells characterized by formation of cytoplasmic vacuoles derived from lysosomes. *Cancer Sci.* **2020**, *111*, 2132–2145. [[CrossRef](#)]
76. Zhang, J.; Wang, Y.; Liu, X.; Dagda, R.K.; Zhang, Y. How AMPK and PKA interplay to regulate mitochondrial function and survival in models of ischemia and diabetes. *Oxid. Med. Cell. Longev.* **2017**, *2017*, 1. [[CrossRef](#)] [[PubMed](#)]
77. Ohanna, M.; Giuliano, S.; Bonet, C.; Imbert, V.; Hofman, V.; Zangari, J.; Bille, K.; Robert, C.; Bressac-de Paillerets, B.; Hofman, P.; et al. Senescent cells develop a parg-1 and nuclear factor- κ B-associated secretome (PNAS). *Genes Dev.* **2011**, *25*, 1245–1261. [[CrossRef](#)] [[PubMed](#)]
78. Arisan, E.D.; Rencuzogullari, O.; Coban, M.; Sevgin, B.; Obakan-Yerlikaya, P.; Çoker-Gürkan, A.; Palavan-Unsal, N. The role of the PI3K/AKT/mTOR signaling axis in the decision of the celastrol-induced cell death mechanism related to the lipid regulatory pathway in prostate cancer cells. *Phytochem. Lett.* **2020**, *39*, 73–83. [[CrossRef](#)]
79. Yuedi, D.; Houbao, L.; Pinxiang, L.; Hui, W.; Min, T.; Dexiang, Z. KLF2 induces the senescence of pancreatic cancer cells by cooperating with FOXO4 to upregulate p21. *Exp. Cell Res.* **2020**, *388*, 111784. [[CrossRef](#)]